Clinical Neurophysiology 130 (2019) 491–504

Contents lists available at ScienceDirect

Clinical Neurophysiology

journal homepage: www.elsevier.com/locate/clinph

Assessing the localization accuracy and clinical utility of electric and magnetic source imaging in children with epilepsy

Eleonora Tamilia [a,b,1], Michel AlHilani [a,b,1], Naoaki Tanaka [c,d], Melissa Tsuboyama [e], Jurriaan M. Peters [e], P. Ellen Grant [b], Joseph R. Madsen [f], Steven M. Stufflebeam. [c], Phillip L. Pearl [e], Christos Papadelis [a,b,*]

[a] Laboratory of Children's Brain Dynamics, Division of Newborn Medicine, Boston Children's Hospital, Harvard Medical School, Boston, MA, USA
[b] Fetal-Neonatal Neuroimaging Developmental Science Center, Boston Children's Hospital, Harvard Medical School, Boston, MA, USA
[c] Athinoula A. Martinos Center for Biomedical Imaging, Massachusetts General Hospital, Harvard Medical School, Boston, MA, USA
[d] Sapporo Neuroimaging Research Group, Sapporo, Japan
[e] Division of Epilepsy and Clinical Neurophysiology, Department of Neurology, Boston Children's Hospital, Harvard Medical School, Boston, MA, USA
[f] Division of Epilepsy Surgery, Department of Neurosurgery, Boston Children's Hospital, Harvard Medical School, USA

ARTICLE INFO

Article history:
Accepted 8 January 2019
Available online 31 January 2019

Keywords:
Epilepsy surgery
Source localization
Irritative zone
Magnetoencephalography
EEG
Intracranial EEG

HIGHLIGHTS

- 306-channel MEG localizes the irritative zone more accurately than 21- and 72-channel EEG.
- Proximity of both magnetic and electric source imaging to the resection is linked to outcome.
- Resection of the irritative zone localized using MEG helps predicting the patient's outcome.

ABSTRACT

Objective: To evaluate the accuracy and clinical utility of conventional 21-channel EEG (conv-EEG), 72-channel high-density EEG (HD-EEG) and 306-channel MEG in localizing interictal epileptiform discharges (IEDs).
Methods: Twenty-four children who underwent epilepsy surgery were studied. IEDs on conv-EEG, HD-EEG, MEG and intracranial EEG (iEEG) were localized using equivalent current dipoles and dynamical statistical parametric mapping (dSPM). We compared the *localization error* (E_{Loc}) with respect to the *ground-truth Irritative Zone (IZ)*, defined by iEEG sources, between non-invasive modalities and the distance from resection (D_{res}) between good- (Engel 1) and poor-outcomes. For each patient, we estimated the *resection percentage* of IED sources and tested whether it predicted outcome.
Results: MEG presented lower E_{Loc} than HD-EEG and conv-EEG. For all modalities, D_{res} was shorter in good-outcome than poor-outcome patients, but only the *resection percentage* of the *ground-truth* IZ and MEG-IZ predicted surgical outcome.
Conclusions: MEG localizes the IZ more accurately than conv-EEG and HD-EEG. MSI may help the presurgical evaluation in terms of patient's outcome prediction. The promising clinical value of ESI for both conv-EEG and HD-EEG prompts the use of higher-density EEG-systems to possibly achieve MEG performance.
Significance: Localizing the IZ non-invasively with MSI/ESI facilitates presurgical evaluation and surgical prognosis assessment.

1. Introduction

Childhood epilepsy is a common neurological disorder with a prevalence rate of 4–6 per 1000 children (Cowan et al., 1989), and has a major impact on children's development (Bailet and Turk, 2000). A large proportion (~30%) of pediatric patients with epilepsy become medically intractable and require resective neurosurgery that can lead to a significant reduction of seizures or seizure freedom (Ryvlin et al., 2014; Shah et al., 2015). To be successful, epilepsy surgery requires a comprehensive preoperative evaluation to define the epileptogenic zone (EZ), the brain region that is indispensable for the generation of seizures, while preserving the eloquent tissue, which includes the cortical

* Corresponding author at: Boston Children's Hospital, Harvard Medical School, 300 Longwood Ave, Boston, MA 02115, USA. Fax: +1 781 216 1172.
E-mail address: christos.papadelis@childrens.harvard.edu (C. Papadelis).
[1] These authors contributed equally.

https://doi.org/10.1016/j.clinph.2019.01.009
1388-2457/

areas related to given functions (such as visual, language or motor), to avoid unacceptable deficits for the patient (Rosenow and Lüders, 2001).

Due to a lack of tools and methods that directly measure the EZ, this area is estimated indirectly through a variety of diagnostic tools that allow defining different cortical zones (Rosenow and Lüders, 2001), each of which is an estimate of the EZ. To this purpose, non-invasive electrophysiological tests are often performed, which include the conventional EEG (conv-EEG) (whereby 19–21 electrodes are typically applied to the scalp), as well as more sophisticated tests, such as the high-density EEG (HD-EEG) and the magnetoencephalography (MEG). These tests allow the localization of the irritative zone (IZ) (Mégevand and Seeck, 2018), the brain area that generates interictal epileptiform discharges (IEDs) (Rosenow and Lüders, 2001), through electric or magnetic source imaging (ESI/MSI). When the non-invasive tests are inconclusive or unable to determine a definite epileptogenic area to resect, intracranial EEG (iEEG) is performed before a final surgical decision can be made. Yet, iEEG recordings are costly, require a cooperative patient, carry surgical risks including hemorrhage, bleeding, or injury from implantation (Önal et al., 2003), and may lead to errors of omission since they leave large areas of the brain unexplored. These intrinsic iEEG limitations may ultimately reduce the number of epilepsy patients who are offered surgery.

The noninvasive localization of the epileptogenic focus through ESI or MSI plays a fundamental role for patients with medically refractory epilepsy (MRE), since it obviates the need for invasive procedures or, in more complex clinical cases, can optimize their planning. A growing body of literature has investigated the contribution of ESI/MSI during the surgical work-up of patients with MRE by evaluating their localization accuracy and clinical utility. The accuracy with which the ESI or MSI can localize the IZ has been estimated in several previous studies, which used indirect estimates of the IZ as ground-truth, such as the seizure onset zone (SOZ) defined by iEEG (MSI: Almubarak et al., 2014; Englot et al., 2015; Knowlton et al., 2006, 2008a; Murakami et al., 2016; ESI: Abdallah et al., 2017; Rikir et al., 2014) or the anatomical area of MRI abnormality (MSI: Englot et al., 2015; Ossenblok et al., 2007; Pellegrino et al., 2018; Stefan et al., 2003; ESI: Diekmann et al., 1998; Lantz et al., 2003; MSI/ESI: Bast et al., 2004; Nakasato et al., 1994). Other studies utilized a direct estimate of the ground-truth, given by the iEEG-defined IZ: they evaluated the concordance of the ESI/MSI localization with the lobar/sublobar region indicated by the iEEG contacts showing IEDs (ESI: Gavaret et al., 2009; Nakasato et al., 1994; Song et al., 2015; MSI: Bouet et al., 2012; Huiskamp et al., 2010; Nakasato et al., 1994; Tanaka et al., 2018a; MSI/ESI: Leijten et al., 2003; Park et al., 2015). Only a few studies used a quantitative measure (i.e. distance) to estimate the ESI/MSI accuracy to the ground-truth IZ, reporting distances of ~15 mm for ESI (Birot et al., 2014; Mégevand et al., 2014) and 9 mm for MSI (Kim et al., 2016). In these cases, the ground-truth IZ was defined by the location of the most active iEEG contacts. Yet, for subdural contacts, which lie on the gyral crowns of the brain, the location of the recording iEEG contact differs from the actual location of the underlying source, if this is located in the depth of the sulcus (Ramantani et al., 2013). To our best knowledge, only one study so far compared the location of MSI/ESI solutions from MEG and scalp EEG with the actual location of the IEDs sources localized with ESI using electrocorticography (ECoG) (Nakasato et al., 1994), and showed an agreement at the lobar level more consistently for MEG than EEG. Yet, the results of this study were limited by a small sample (six patients) and a low number of channels (41-channel EEG; 7-channel MEG; and 48-channel ECoG). Thus, despite these previous efforts, there is a lack of quantitative studies assessing the accuracy of conv-EEG, HD-EEG, and MEG to localize the IZ with respect to the ground-truth given by the actual location of iEEG sources. Improving the 3D demarcation of the *ground-truth IZ* using ESI on iEEG data would allow direct comparison of the epileptic generators estimated via non-invasive and invasive techniques at the source level. Finally, there is a paucity of studies that examine the clinical utility of these three electrophysiological tests with respect to the gold standard of seizure freedom after resection in the same cohort of patients, despite several investigations on this topic (MSI: Almubarak et al., 2014; Englot et al., 2015; Kim et al., 2013; Knowlton et al., 2006, 2008b; Murakami et al., 2016; Stefan et al., 2003; Tanaka et al., 2018b; ESI: Birot et al., 2014; Brodbeck et al., 2011; Lascano et al., 2016; Mégevand et al., 2014; Russo et al., 2016; ESI/MSI: Bast et al., 2004).

The main goal of this study is to quantitatively assess and compare the accuracy of conv-EEG, HD-EEG and MEG in localizing IEDs prior to epilepsy surgery in children with MRE, and to determine the clinical utility of ESI/MSI against the gold standard of seizure freedom after resection. To pursue our goal, we: (i) localized with ESI the IED sources using conv-EEG (21–25 channels EEG, manually co-registered with patient's MRI without head tracking) and HD-EEG (72 channels EEG, co-registered with patient's MRI via head tracking); (ii) localized with MSI the sources of IEDs using MEG (306 sensors, co-registered with patient's MRI via head tracking); (iii) defined the *ground-truth IZ* at the source level using ESI on iEEG recordings, thus improving its 3D demarcation; (iv) compared the *localization error* (E_{Loc}) and *precision* of the ESI and MSI solutions with respect to the *ground-truth IZ*, considering also the distinction between IEDs that were concurrent on HD-EEG and MEG from those unique to one modality; (iv) compared the distances of the ESI and MSI solutions from the surgically resected volume between patients with good and poor outcome and (v) evaluated whether the resection of the regions indicated by the ESI/MSI findings in each patient predicts the surgical outcome.

2. Methods

2.1. Patient cohort

We retrospectively reviewed the data of 638 patients with MRE who underwent presurgical evaluation at the Epilepsy Center of Boston Children's Hospital (BCH) between April 2010 and October 2016. From this cohort, we selected patients who met the following criteria: (i) underwent simultaneous MEG/HD-EEG examination; (ii) underwent long-term monitoring with iEEG (grids, strips, and/or depth electrodes); (iii) had post-implantation computerized tomography (CT) scan and pre-operative MRI; (iv) underwent surgical resection after iEEG monitoring; and (v) had ≥12 months of postsurgical follow-up. Exclusion criteria were absence of IEDs on MEG/HD-EEG or iEEG or presence of extensive artifacts in the MEG or EEG recordings. The study protocol received approval by the BCH Institutional Review Board (IRB-P00022114), which waived the need for written informed consent due to the study's retrospective character.

2.2. Conventional EEG recordings

All patients underwent conventional long-term video-EEG recording in the Clinical Neurophysiology Laboratory of BCH using the standard clinical EEG setup with 19 electrodes, plus two additional fronto-temporal leads (FT9 and FT10) and four optional electrodes in some cases (F9, F10, P9, P10). Data were recorded using the XLTEK EMU40 system (Natus Inc., USA) with a sampling rate of 1024 Hz. Individual leads (gold cups) were placed according to the international 10/20 system. Impedances were kept below 10 KΩ during the entire recording session. Reference and ground

electrodes were placed in frontocentral areas (near FC1 and FC2, respectively).

2.3. Simultaneous HD-EEG and MEG recordings

Simultaneous MEG/HD-EEG recordings were conducted at the MEG Core Laboratory of Athinoula Martinos Center for Biomedical Imaging (Charlestown, MA). The followed procedures were in accordance with the International Federation of Clinical Neurophysiology (Hari et al., 2018) and the American Clinical MEG Society guidelines (Bagic et al., 2011). The recordings were performed in a three-layer magnetically shielded room (Imedco, Hägendorf, Switzerland) with a whole-head 306-sensor system (VectorView, Elekta Neuromag, Helsinki, Finland), consisting of 204 planar gradiometers and 102 magnetometers over 102 locations. Simultaneous HD-EEG was recorded using a non-magnetic 70-channel electrode cap (EASYCAP, Herrsching, Germany) where the electrodes were positioned following the 10–10 system. Two additional EEG electrodes were also positioned on the temporal regions (T1/T2). Nose reference was used (Hari and Puce, 2017). Four head position indicator (HPI) coils were placed on the head. The relative locations of the HPI coils and EEG electrodes with respect to anatomical landmarks on patient's head were determined using a three-dimensional (3D) digitizer. This allowed aligning the MEG, EEG, and MRI coordinate systems. Additional electrodes were also placed to measure horizontal and vertical electrooculography (EOG) and electrocardiography (ECG). The recordings were performed in supine position. Patients were partially sleep deprived and instructed to rest or sleep during the recording. Spontaneous MEG/HD-EEG signals were recorded for 10–12 recording sessions per patient (4–5 min each) with a sampling rate of 1000 Hz and an online low-pass Infinite Impulse Response (IIR) filter of 6^{th} order at 400 Hz. Head position was measured before the beginning of each session. More details about the protocol are provided in our previous studies (Knake et al., 2006; Papadelis et al., 2016).

2.4. Long-term iEEG recordings

Invasive monitoring was performed after consensus of a multidisciplinary epilepsy surgery team due to a perceived need for a better definition of the SOZ and/or the functional regions. Intracranial EEG was recorded with subdural grids and strips (2.3-mm exposure diameter, 10-mm distance; Ad-Tech., USA) and/or depth electrodes (10 linearly arranged contacts: 1.1-mm diameter, 3–5 mm inter-distance; Ad-Tech., USA), using XLTEK NeuroWorks (Natus Inc., USA) with a sampling rate ranging between 500 and 2000 Hz. The location, number and type of electrodes were decided to monitor all possible epileptogenic areas regarded "of interest" based on the patient's presurgical evaluation, which included ictal video-EEG, MRI and MEG. The ESI/MSI findings reported here were performed retrospectively and blind to previous clinical findings; thus, they did not influence surgical coverage planning.

2.5. MRI and CT

Anatomical MRIs were acquired before and after surgical resection with magnetization-prepared rapid acquisition gradient-echo sequences (MPRAGE; TE = 1.74 ms, TR = 2, 520 ms, voxel size = $1 \times 1 \times 1$ mm). The scans were obtained using a high resolution 3 T scanner (TIM TRIO, Siemens AG, Erlangen, Germany). More details about the MRI scanning protocol can be found elsewhere (Prabhu and Mahomed, 2015). For HD-EEG/MEG recordings, co-registration between the MRI and the head points digitized from the patient at the time of the acquisition was performed using *Brainstorm* (Tadel et al., 2011). For conv-EEG, no head tracking data had been collected. Thus, the EEG channel locations were manually co-registered with the patient's MRI based on the MNI coordinates of the 10–20 system, as defined on the default Colin27 brain (Holmes et al., 1998). Furthermore, we determined the anatomical location of each iEEG contact by co-registering the post-implantation CT (voxel size = $0.5 \times 0.5 \times 0.5$ mm) with the preoperative MRI using *Brainstorm* (Tadel et al., 2011). Each contact coordinate was determined from the co-registered CT-MRI image by reviewing sagittal, coronal, and axial planes and was mapped on the patient's 3D cortical surface reconstructed from the preoperative MRI using *FreeSurfer* (Dale et al., 1999).

2.6. Clinically-defined SOZ

The SOZ was prospectively determined during the long-term iEEG monitoring. Pediatric epileptologists identified the iEEG contact/s showing the earliest change from background activity associated with each captured clinical seizure (*SOZ contacts*), independently from this study. For each patient, we determined the SOZ location as the location of all *SOZ contacts*.

2.7. Selection of interictal data for conv-EEG, HD-EEG, MEG and iEEG

As part of the conv-EEG and iEEG long-term monitoring at BCH, pediatric neurophysiologists extracted multiple 5–10 min segments of data with considerable IEDs on a daily basis. For the purpose of this study, two pediatric clinical neurophysiologists (M.T. and J.M.P.), blinded to the resection and the surgical outcome, retrospectively reviewed these segments and selected, for each patient, the first 5–10 min of data, without including major artifacts, technical disruptions or ictal events. HD-EEG\MEG data were reviewed by a pediatric epileptologist (N.T.) who extracted three 4-min sessions that contained considerable IEDs. These 12-min data were used after excluding major artifacts or technical disruptions.

2.8. Identification of IEDs

For all modalities, channels with continuous artifacts or obvious noise were excluded. IEDs were identified on filtered data (band-pass filter: 1–70 Hz; notch filter: 60 Hz and harmonics) through visual inspection of pediatric epileptologists or MEG experts (M.T. and J.M.P. for EEG; N.T. and C.P. for MEG), who were blind to each other's markings and to each patient's history. IED marking was performed independently for each modality, according to the following established criteria (Chatrian, 1974): (i) paroxysmal occurrence; (ii) abrupt change in polarity; (iii) duration < 200 ms; and (iv) scalp topography consistent with a physiologic field. Average montage was applied to iEEG, while both average and bipolar montages were applied to conv-EEG and HD-EEG. For MEG, the Signal Space Projection (SSP) technique was used to reject external disturbances (Uusitalo and Ilmoniemi, 1997) due to cardiac events detected by ECG. The 306 sensors were divided into eight regions including 38–39 channels each (right- and left-temporal, right - and left-frontal, right and left-parietal, right - and left-occipital), and IEDs marking was performed region by region. Similarly, for iEEG, the channels from the same grid, strip or depth electrode were inspected together. For all modalities, the reviewers marked the peak of the main spike deflection (i.e. the earliest or the most prominent according to the reviewer's judgment), excluding any portion contaminated by biological artifacts (e.g. heartbeat or eye movements visible on ECG or EOG). Only IEDs that were marked by both reviewers were used for further analysis. For the simultaneous MEG/HD-EEG data, the IEDs that occurred simultaneously on both modalities were identified as *concurrent* (Fig. 1A) as opposed to *HD-EEG-only* (Fig. 1B) or *MEG-only* IEDs (Fig. 1C). For each modality, we calculated the rate of IEDs per patient (number of IEDs divided by the data duration; IEDs/min).

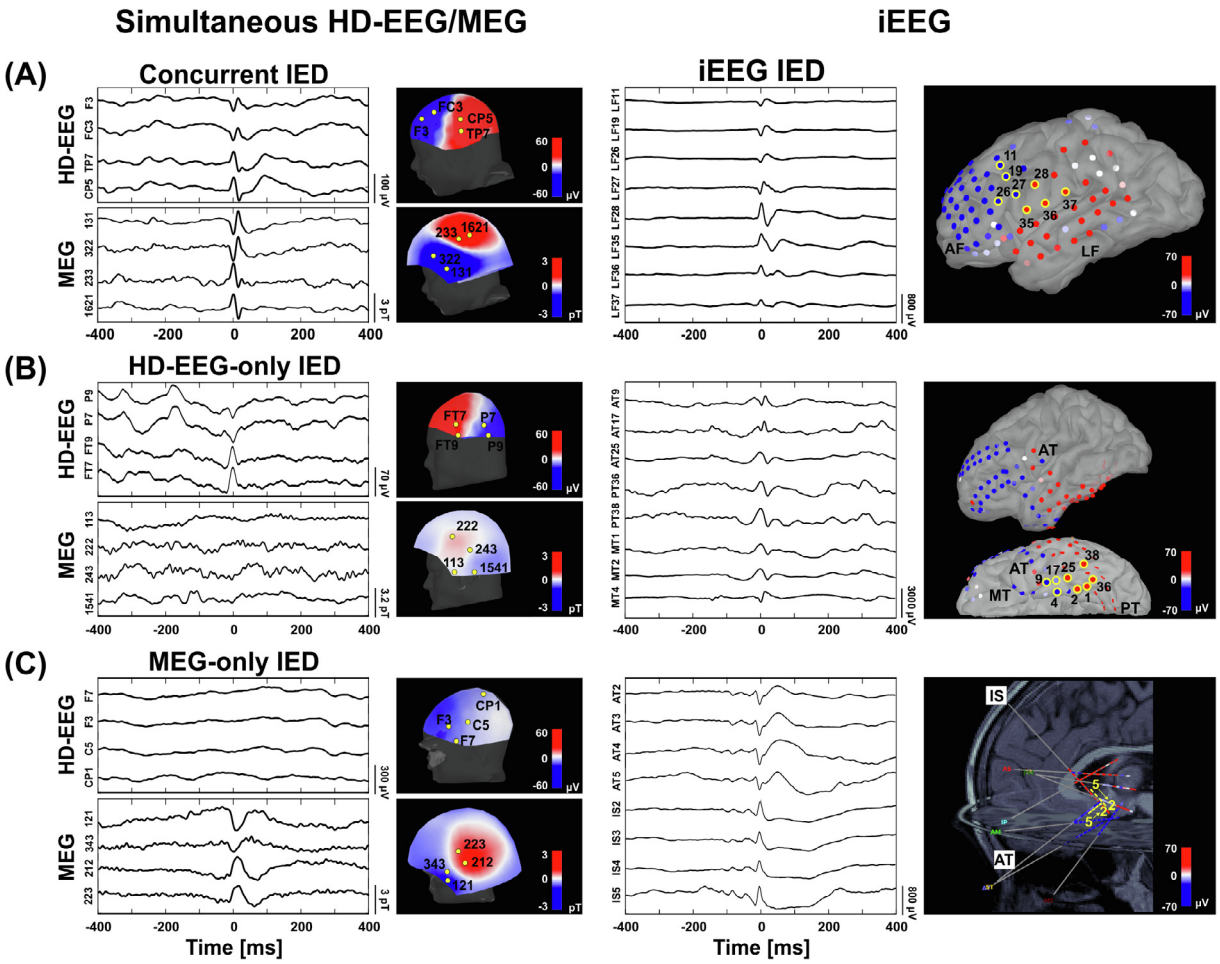

Fig. 1. IEDs on HD-EEG/MEG and iEEG data. (A) Example of *concurrent* IED on simultaneous HD-EEG/MEG. Data from patient #21 (9-year-old girl with chronic focal encephalitis in the left hemisphere). On the left, simultaneous HD-EEG and MEG data (800 ms) filtered between 1 and 70 Hz. Topographic maps of the magnetic field and electrical potential (perpendicular between HD-EEG and MEG) show a polarity change between electrodes F3-FC3 and TP7-CP5, and between magnetometers/gradiometers 131–322 and 233–1621. On the right, example of IED on iEEG [lateral frontal (LF) grid] from same patient. Topographic maps indicate a polarity change between contacts LF1-19-26-27 and LF28-35-36-37. Polarity changes for both the non-invasive (i.e. MEG and HD-EEG) and invasive (iEEG) recordings indicate an underlying focal dipolar source in left frontotemporal regions. (B) Example of IED that occurs only in HD-EEG *(HD-EEG only)*. Data from patient #9 (15-year-old boy with left temporal focal cortical dysplasia). On the left, simultaneous HD-EEG and MEG data filtered between 1 and 70 Hz. Topographic map of electric potentials shows a polarity change between electrodes P9-P7 and electrodes FT9-FT7. No change in polarity is seen on the topographic map of the magnetic potential. On the right, example of IED on iEEG [anterior temporal (AT), posterior-temporal (PT) and mesial-temporal (MT) grid] from same patient. Topographic maps indicate a polarity change between contacts AT9-AT17-MT4 and AT25-PT38-MT1-MT2. Polarity changes for both HD-EEG and iEEG recordings indicate an underlying focal dipolar source in left temporal region. (C) Example of *MEG-only* IED. Data from patient #2 (6-year-old girl with left temporal focal cortical dysplasia). On the left, simultaneous HD-EEG and MEG data (filtered: 1–70 Hz). Topographic map of magnetic potentials shows a polarity change between magnetometers/gradiometers 121–343 and 212–223. No change in polarity is seen on the topographic map of the electric potential. On the right, example of IED on iEEG [anterior temporal (AT) and insular (IS) depth] from same patient. Topographic map indicates a polarity change between contacts AT2-AT3-AT4-AT5 and IS2-IS3-IS4-IS5. Polarity changes for both MEG and iEEG recordings indicate an underlying focal dipolar source in deep left anterior temporal region.

2.9. Source localization of IEDs

2.9.1. Forward model

We constructed a realistic head model from each patient's pre-operative MRI with *OpenMEEG* software (Gramfort et al., 2010). The individual cortical surfaces were extracted from the MRI volume using the automatic segmentation pipeline in *Freesurfer* with default parameter settings (Dale et al., 1999). For conv-EEG, HD-EEG and MEG, we used a three-layer (scalp, outer skull, and inner skull) boundary elementary model (BEM), while for iEEG we used a one-layer (inner skull) BEM model (layer thickness: 4 mm). A grid of points that sampled the full brain volume (*volume points*) was generated using the adaptive integration method in *Brainstorm* (Tadel et al., 2011), in order to also account for deeper or sub-cortical brain regions.

2.9.2. Equivalent Current Dipoles (ECDs)

We localized the underlying generator of each IED using the ECD model (Hamalainen et al., 1993), which is the only validated and approved method for clinical use (Barth et al., 1982; Knowlton et al., 1997; Stefan et al., 2003). Unconstrained source analysis was performed in the volume space at the peak of each IED using a dipole scanning method, which searches iteratively for the dipole explaining the best the recordings without any a priori definition of the initialization point. We localized each individual IED as opposed to their average to avoid the inherent risk of merging IEDs with similar scalp topography even though generated by different sources (Diekmann et al., 1998; Rikir et al., 2014). Fig. 2 shows an example of ECD findings for all neuroimaging modalities (i.e. conv-EEG, HD-EEG, MEG, and iEEG) in a 13-year-old boy with MRE from our cohort (patient #5). Only dipoles

with a goodness-of-fit (GOF) higher than 60% were accepted for further analysis. Each dipole was classified as either *clustered* or *scattered*. A cluster was defined as a group of at least five dipoles (Almubarak et al., 2014) located within a 15-mm distance. All other dipoles, not belonging to any cluster, were classified as *scattered*. When multiple clusters were identified, all of them were considered in our analysis.

2.9.3. Dynamical Statistical Parametric Mapping (dSPM)

Each IED was also localized using dSPM (Dale et al., 2000), a distributed source-modeling technique which assumes that the observed EEG or MEG activity can be generated by extended sources over the brain volume. For each modality, we determined the location of the sources underlying the peak of each IED (volume points showing >90% of the maximum dSPM value). Then, for each patient, the sources of all IEDs were merged in a single dSPM solution. Fig. 2 shows an example of the dSPM findings for all neuroimaging modalities for patient #5.

2.10. Resection and postsurgical outcome

The resection margins were determined based on the patient's presurgical evaluation and long-term iEEG monitoring, with the aim of removing the SOZ and the regions that are particularly active during interictal periods. The location of the eloquent cortex and/or vascular structures was also considered and could limit the complete resection of the EZ. The exact location and extent of the resected volume were determined by co-registering the patient's presurgical and postsurgical MRIs. We defined the resected volume by marking all the volume points of the presurgical MRI corresponding to the resection cavity on the co-registered postsurgical MRI. The percentage of resected volume over the entire brain volume was estimated for each patient. The distance of the SOZ from the resection was calculated as the Euclidean distance between each SOZ contact and the closest resected volume point. Then, the *resection percentage* of the SOZ was estimated as the percentage of SOZ contacts within 15 mm from the resection. Postsurgical outcome was evaluated by a board-certified pediatric epileptologist (J. M.P.) from the most recent follow-up visit using the Engel scale (Engel et al., 1993). We dichotomized the outcome into good (Engel 1) and poor (Engel $\geq$ 2).

2.11. Validation of the IED sources localized via conv-EEG, HD-EEG, and MEG

2.11.1. Validation against iEEG-defined ground-truth IZ and SOZ

Given the partial coverage of iEEG, the validation against *ground-truth IZ* and SOZ was carried out only for the sources localized within the regions covered by the iEEG (Fig. 3A). The validation was carried out similarly for dipole and dSPM solutions, independently. For each IED source (dipole or dSPM), we calculated the distance from the iEEG coverage (D_{cov}), as the Euclidean distance from the closest iEEG contact (white arrow in Fig. 3A). The IED sources with $D_{cov} > 30$ mm were classified as *outside-coverage* (Fig. 3A, red dipole), or *within-coverage* otherwise (green dipoles in Fig. 3). Then, for each non-invasive modality (conv-EEG, HD-EEG and MEG), we estimated the *localization error* (E_{Loc}) with respect to the *ground-truth IZ* given by the IED sources localized via iEEG (light blue dipoles in Fig. 3B). The E_{Loc} was calculated as the Euclidean distance of each IED source from the closest point of the *ground-truth IZ* (cyan arrow in Fig. 3C). Sources with $E_{Loc} \leq 15$ mm were classified as *concordant* with the *ground-truth IZ* (blue dipole in Fig. 3C) or *non-concordant* otherwise (orange dipole in Fig. 3C), as in the quantitative study of Kim et al. (2016). This

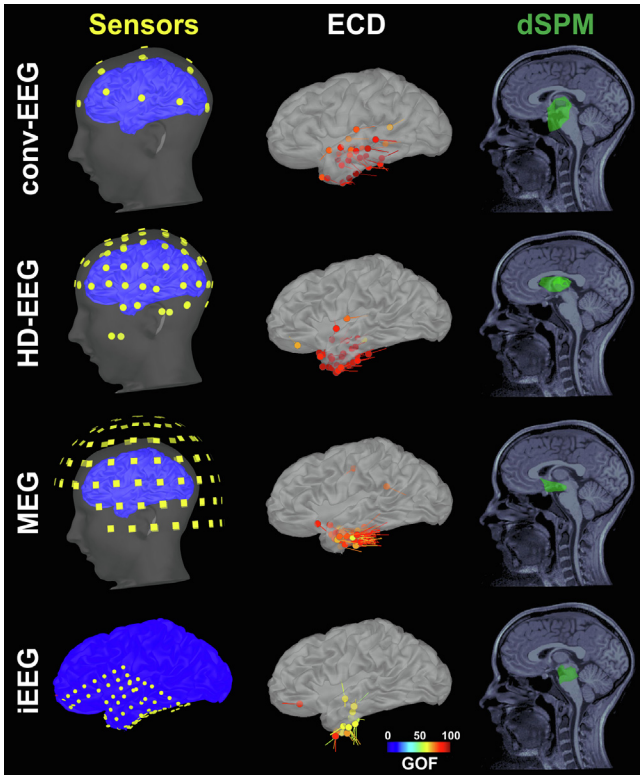

Fig. 2. Sensor locations and source localization of IEDs with ECD and dSPM in a patient with MRE for all four modalities (non-invasive: conv-EEG, HD-EEG, and MEG; invasive: iEEG). *Left*: Location of sensors for each modality co-registered with the patient's cortical surface (patient #5) reconstructed from pre-operative MRI. From top to bottom: conv-EEG (21 electrodes), HD-EEG (72 electrodes), MEG (102 locations where 306 sensors are distributed) and iEEG (72 subdural contacts). For conv-EEG, co-registration between the EEG and MRI was performed manually without digital information from a head position tracking system. For MEG/HD-EEG, co-registration between the MEG/HD-EEG and MRI was performed using a 3D Fastrak digitizer to track the location of the head localization coils and EEG electrodes. For iEEG, the location of the contacts was determined by co-registering the presurgical MRI and post-implantation CT scan. *Middle*: Source localization of the IEDs using ECDs for each different modality. ECDs are color-coded based on their goodness of fit (GOF). Only accepted dipoles (GOF > 60%) are displayed (conv-EEG: 24 dipoles; HD-EEG: 39 dipoles; MEG: 67 dipoles; iEEG: 13 dipoles). *Right*: Source localization of the IEDs using dSPM for each different modality. The dSPM was calculated for each IED. All IEDs were then merged in order to generate a single dSPM map (green volume) per patient per modality.

15-mm cut-off was defined based on the mean width of the parahippocampal gyrus (Ono et al., 1990), and suggests that two sources were close to each other within the distance of gyral width even if not necessarily located in the same gyrus (Kim et al., 2016). The *precision* of each modality with respect to the *ground-truth IZ* was estimated at the gyral-width level as percentage of *concordant* sources out of those *within-coverage*. Furthermore, we calculated the Euclidian distance of each IED source from the closest *SOZ contact* (D_{SOZ}, Fig. 3D). The *concordance* of each modality to the SOZ was estimated as percentage of *within-coverage* dipoles or dSPM sources with $D_{SOZ} \leq 15$ mm.

2.11.2. Validation against resection and outcome

For all modalities, we calculated the distance from resection (D_{res}) of each IED source as their Euclidian distance from the closest point of the resected volume, as shown in Fig. 3E. IED sources with a $D_{res} \leq 15$ mm were classified as *resected*. For each individual patient, we estimated the percentage of the IZ that was resected (*resection percentage*) for all different modalities.

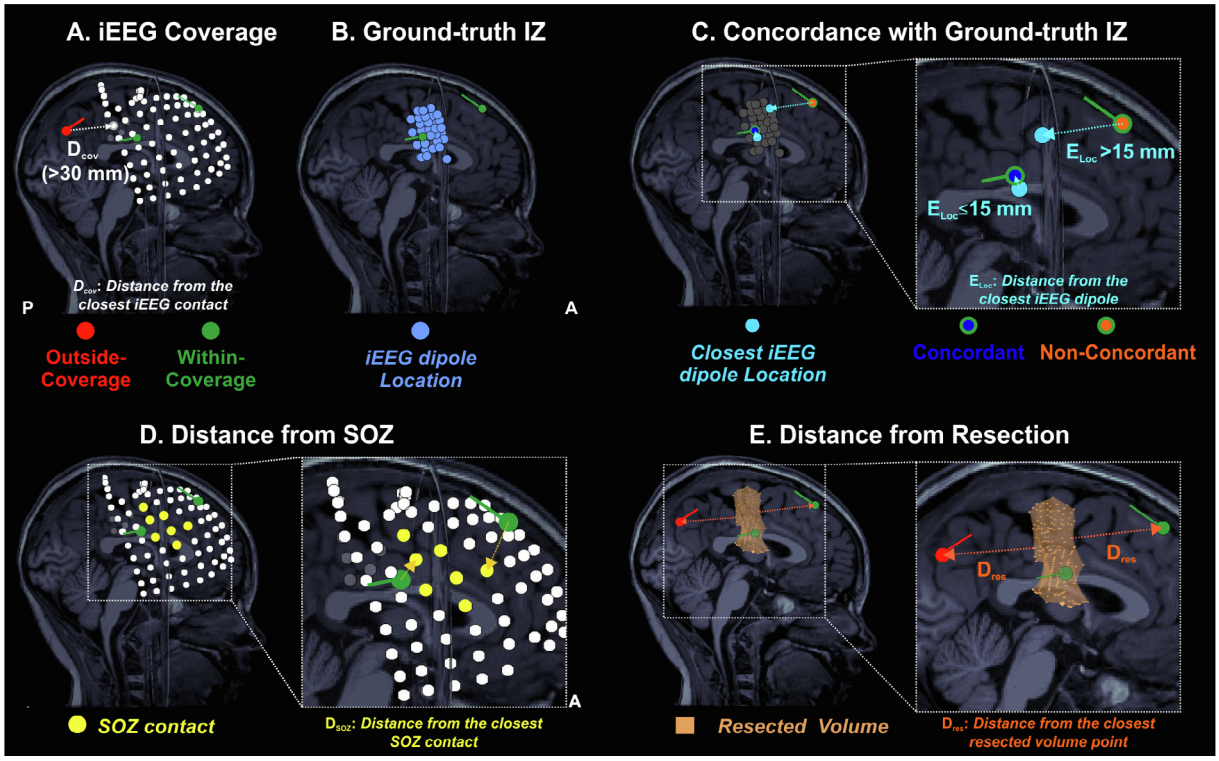

Fig. 3. Estimation of Localization Error (E_{loc}), distance from the SOZ (D_{SOZ}) and Distance from Resection (D_{res}). (A) Non-invasively estimated dipoles are classified as *outside-coverage* ($D_{cov} \geq 30$ mm, red dipole) or *within-coverage* ($D_{cov} \leq 30$ mm, green dipole) based on their Euclidean distance (D_{cov}, white arrow) from the closest iEEG contact (white dots). MRI is displayed from posterior (P) left to anterior (A) right. (B) *Ground-truth IZ* is defined by the dipoles localized from the iEEG data. Light blue dots mark each iEEG dipole location. (C) *Within-coverage* dipoles are classified as *concordant* (blue) or *non-concordant* (orange) based on their localization error (E_{loc}). E_{loc} is the Euclidean distance (cyan arrows) from the location of the closest iEEG dipole (cyan dot). (D) Distance of each *within-coverage* dipole from the SOZ (D_{SOZ}) is calculated as its Euclidian distance the closest *SOZ contact* (yellow). (E) Distance of each dipole from the resection cavity is defined by the Euclidean distance of each dipole from the closest points of the resected volume (D_{res}, orange arrow). The resected volume (orange volume) is defined by marking the volume points corresponding to the resection cavity on the postsurgical MRI co-registered with the presurgical MRI.

2.12. Concordance of HD-EEG and MEG with other presurgical methods

To evaluate the added value of HD-EEG and MEG with respect to other presurgical methods, we compared the HD-EEG and MEG findings with the reference regions pointed out by presurgical ictal EEG and MRI reports. When no ictal EEG was captured or MRI was normal, their results were classified as negative. The concordance of the HD-EEG and MEG regions with each reference region was determined at the lobar level (Nissen et al., 2016; Velmurugan et al., 2018) as follows: (i) *concordant specific* (HD-EEG/MEG lobe/s included within the reference lobe/s); (ii) *concordant nonspecific* (HD-EEG/MEG lobe/s within and outside the reference lobe/s); (iii) *discordant* (HD-EEG/MEG lobe/s different from the reference lobe/s). Finally, we also evaluated the lobar concordance of the ictal EEG and MRI lesion with respect to the resected region.

2.13. Statistical analysis

We used Wilcoxon signed-rank test to compare IED rates between modalities. Mixed-effect analysis of variance (ANOVA) was used to compare the E_{loc}, D_{SOZ} and D_{res} between different modalities (or source localization methods) with random effects to correct for repeated measurements within patients. Additionally, Wilcoxon rank-sum was used to compare the E_{loc} between modalities for each individual patient. For each modality, two-sample *t*-test was used to compare D_{res} between good and poor outcome patients. To test whether the ESI/MSI solutions can predict the patient's outcome, we used a logistic regression model of the probability of good outcome as function of the ESI/MSI *resection percentage* for each modality. Logistic regression was also used to assess the predictive effect of the brain resected volume and SOZ resection on the patients' outcome. Furthermore, Spearman correlation between the *resection percentage* of the SOZ and the ESI/MSI solutions was performed to verify the presence of any relationship between the SOZ resection and the ESI/MSI resection. To compare proportions, χ^2 test (or *Fisher's exact* test, when $n < 5$) was used. A *p*-value of < 0.05 was considered statistically significant. Results are expressed as median (inter-quartile range, IQR) or mean ± standard deviation (SD).

3. Results

3.1. Patient cohort

Twenty-four patients (10 females) matched all the inclusion criteria. Clinical and demographic characteristics of our cohort are reported in Table 1. The mean age at the time of surgery was 11.52 ± 4.27 years (range: 1.8–17.8) and the mean age at epilepsy onset was 4.86 ± 3.65 years (range: 0–15 years). Four patients were excluded from the conv-EEG analysis, because no conv-EEG data were available in the BCH archive. Seventeen patients had an abnormal MRI with different histopathologic diagnoses as indicated in Table 1. Thirteen patients (54%) had good surgical outcome. For two patients (poor outcome), no post-operative MRI was available; thus, they were excluded from all the analyses involving the resection. The type of resection (temporal vs. extra-temporal/multi-lobar, Table 1) was not associated with the

Table 1
Clinical characteristics of our cohort.

No.	Age	Sex	Seizure-onset age	Epilepsy side	MRI Abnormality	Ictal EEG	# iEEG electrodes (SDE + DE)	Resected Lobe(s)	Pathology	Outcome[a]	Post-op Follow-up (months)
1	8.7	M	4	R	Normal	R H	80	F - P	NS	1a	44
2	6.5	Fe	3	L	L T	L FTP	90	Superior T	FCD	1a	14
3	10.25	Fe	8	R	R F	F FP	144 + 10	F	DNET	1a	31
4	9.5	Fe	0.4	L	L T	R H; L FP	140	T	HS; GL	3	13
5	13.5	Fe	10	L	Normal	L T	72	T	FCD	1a	48
6	13	M	9	L	L T	L FTP	72 + 20	T	Tumor	1a	12
7	1.75	M	0.33	R	Multifocal[b]	R FP	112	F	TS	1a	41
8	17.75	Fe	15	L	Normal	L T	88	T	NS	1a	29
9	15.4	M	4	L	Normal	L F	88	T	FCD	2b	25
10	14.75	M	4	L	Normal	L F	88	F	NS	3	36
11	16.25	M	1.5	R	Normal	R H	128	T	NS	3	48
12	8.4	Fe	1	R	R F	R F	112 + 10	F	FCD	1b	42
13	14.7	Fe	6	L	L P	L FP	72	P	FCD	1b	12
14	11.8	M	8	L	L TP	L H; R FP	72 + 30	T - P	NS	2	12
15	12.25	M	7	L	L T	L FT; R F	96	F - T	FCD	3	12
16	12.25	M	0	L	L FTP	L H	238	F - T	FCD	2	37
17	17.5	M	5	L	L F	L FP	64 + 30	F	FCD	1a	13
18	11.4	M	1.5	L	L T	L FTP	96	T	FCD	1a	46
19	16.7	M	5	L	L I	R F; L F	238	T - P	FCD	3	12
20	9.9	M	7	L	L FTP	L FP	64 + 60	P - O	FCD	1b	12
21	8.9	Fe	8	L	L F	L H	96	F - P	CFE	3	25
22	6.4	Fe	4	R	R F	R H	72 + 40	F	FCD	2	31
23	3.8	M	2	R	R F	R FP	128 + 10	F	FCD	1a	12
24	15.2	Fe	3	L	Normal	L FTP	212	F	NS	2	15

M: male, Fe: female, L: left, R: right, SDE: subdural electrodes, DE: depth electrodes, F: Frontal, T: Temporal, P: Parietal, I: Insular, H: Hemisphere, O: Occipital, NS: non-specific, FCD: focal cortical dysplasia, DNET: dysembryoplastic neuroepithelial tumor, HS: hippocampal sclerosis, GL: gliosis, TS: tuberous sclerosis, CFE: chronic focal encephalitis.

[a] According to Engel's classification.

[b] MRI showing multifocal cortical tubers for a patient with TS.

patients' outcome ($p = 0.81$): good outcome was achieved in 63% (n = 5) and 57% (n = 8) of the temporal and extra-temporal/multi-lobar cases respectively. In 11 patients, the overlap of the presumed epileptogenic zone with the eloquent cortex and/or the vascular structures limited the resection of the targeted region, but was not associated with surgical outcome (good-outcome was achieved by six of them). Finally, no association was seen between the presence of an MRI lesion and the outcome ($p = 0.66$).

3.2. IEDs on iEEG, conv-EEG, HD-EEG and MEG

We excluded from the analysis an average of 1.4 ± 1.8 sensors for conv-EEG, 6.8 ± 7.3 sensors for HD-EEG, 3.5 ± 2.1 sensors for MEG, and 0.4 ± 1.2 contacts for iEEG. We identified a total number of 8415 IEDs on iEEG (mean: 351), 829 IEDs on conv-EEG (mean: 41), 2081 IEDs on HD-EEG (mean: 87) and 2922 IEDs on MEG (mean: 122). The rate of IEDs identified on iEEG (48.4 ± 34.2 IEDs/min) was higher than in any other modality ($p < 0.001$). The rate of IEDs on MEG (9.6 ± 13.3 IEDs/min) was higher than the rates on HD-EEG (6.9 ± 9.3 IEDs/min; $p = 0.0285$) and conv-EEG (4.9 ± 5.8 IEDs/min; $p = 0.025$), which did not differ between each other ($p = 0.1651$). In the simultaneous MEG and HD-EEG recordings, we observed a higher percentage of *MEG-only* IEDs (73%) compared to *HD-EEG-only* IEDs (63%; $p < 0.001$): *concurrent* IEDs were identified in 23 patients (96%) with a mean rate of 2.6 ± 3.8 concurrent IEDs/min per patient. The total number of accepted dipoles was 2266 for iEEG (mean: 94), 767 for conv-EEG (mean: 38), 1953 for HD-EEG (mean: 81) and 2171 for MEG (mean: 90). The percentage of dipoles in clusters was different between all modalities ($p < 0.001$), with iEEG showing the highest percentage (95%) followed by MEG (91%), HD-EEG (80%) and conv-EEG (51%). No dipole clusters were found in two cases for iEEG, three cases for MEG and HD-EEG and six cases for conv-EEG. One single cluster was identified in the majority of the cases (iEEG: 68%; conv-EEG: 58%; HD-EEG: 67%; MEG: 86%), while two or three clusters were found in the other cases.

3.3. Concordance of non-invasive ESI and MSI IZ with ground-truth IZ

The proportion of *within-coverage* dipoles differed between MEG, HD-EEG and conv-EEG (Fig. 4A): MEG showed the highest proportion (92%) of *within-coverage* dipoles compared to both HD-EEG (80%; $p < 0.001$) and conv-EEG (70%; $p < 0.001$), which also differed between each other ($p < 0.001$). The majority of the *outside-coverage* dipoles were ipsilateral to the iEEG coverage for both HD-EEG (55%) and MEG (53%), while contralateral for conv-EEG (52%). The E_{Loc} of the MEG dipoles with respect to the *ground-truth IZ* (15.4 ± 12.2 mm) was lower than HD-EEG (19.2 ± 14.2 mm, $p = 0.002$) and conv-EEG dipoles (24.7 ± 14.5 mm, $p = 0.023$), as shown in Fig. 4B. No difference was found between the E_{Loc} of HD-EEG and conv-EEG dipoles ($p = 0.86$). From the comparisons within individual patients, we found that: (i) MEG outperformed HD-EEG in 13 cases (54%) and conv-EEG in nine cases (45%) with a mean improvement of 12 and 13 mm, respectively; (ii) HD-EEG outperformed MEG in 5 cases (21%) and conv-EEG in eight cases (33%) with a mean improvement of 10 and 12 mm, respectively; (iii) conv-EEG outperformed MEG in two cases (10%) and HD-EEG in four cases (20%) with a mean improvement of 13 and 19 mm, respectively; and (iv) no difference was seen between MEG and HD-EEG in six cases (25%), between MEG and conv-EEG in nine cases (45%) and between HD-EEG and conv-EEG in eight cases (40%). Finally, MEG showed the highest precision (59%) to the *ground-truth IZ* (see Fig. 4C) at the gyral-width level compared to both HD-EEG (46%, $p < 0.001$) and conv-EEG (26%, $p < 0.001$), which also differed between each other ($p < 0.001$).

3.3.1. Comparison with distributed source modeling

For MEG and HD-EEG, the proportion of dSPM sources localized *within-coverage* (MEG: 80%; HD-EEG: 63%; $p < 0.001$) was lower than for dipoles (Fig. 4A). For the *within-coverage* sources, we observed that: (i) the dSPM E_{Loc} did not differ from the dipole E_{Loc} for all modalities (Fig. 4B; $p > 0.05$; Table 2); (ii) the dSPM E_{Loc} for

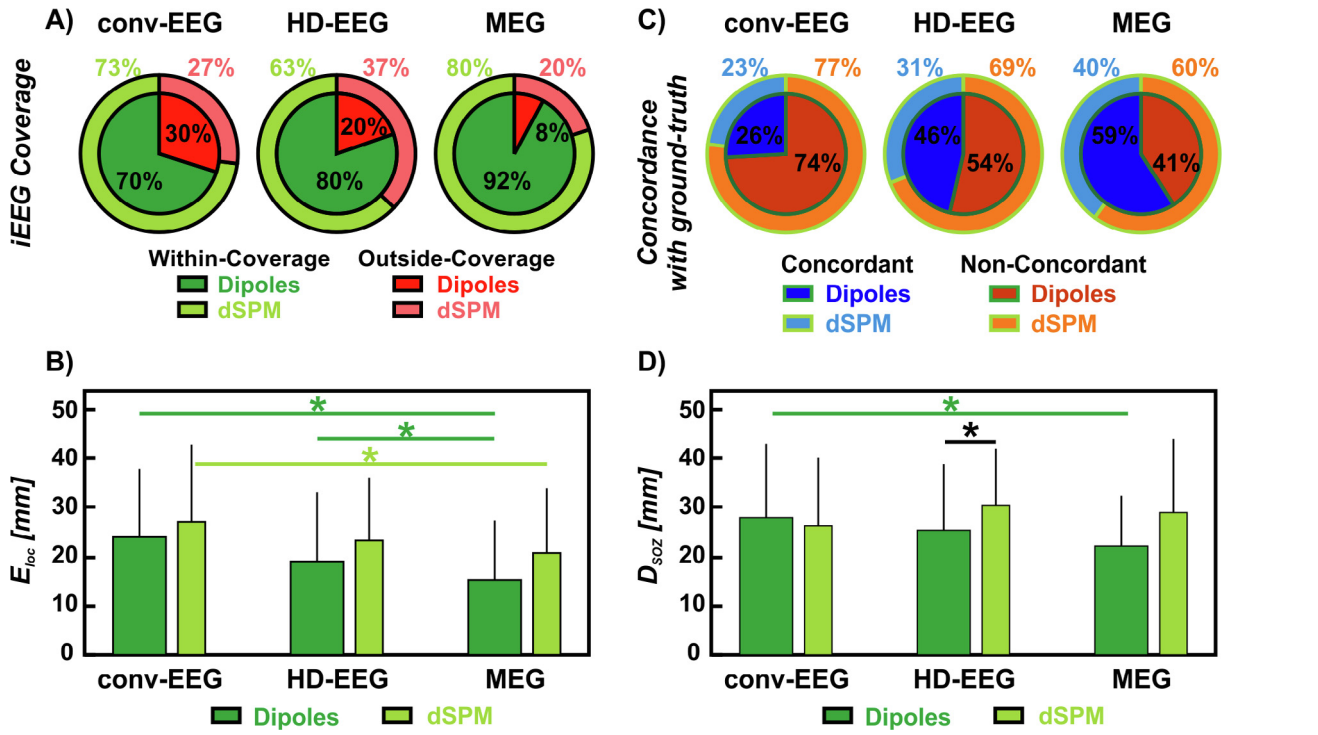

Fig. 4. Non-invasive localization of IEDs (dipoles and dSPM) against ground-truth IZ and SOZ. (A) Red wedges correspond to the proportion of IEDs localized outside iEEG coverage; green wedges correspond to the proportion of IEDs localized within the iEEG coverage. The inner wedges are for dipoles; the outer wedges are for dSPM. (B) Localization error (E_{loc}) of conv-EEG, HD-EEG and MEG with respect to the *ground-truth IZ* (in mm) for both dipoles and dSPM. Difference in E_{loc} was regarded as significant (*) when the *p*-value was <0.05. (C) Blue wedges correspond to the proportion of IED sources concordant with the *ground-truth IZ* at the gyral-width level (out of all the *within-coverage* sources) or *precision*. The orange wedges correspond to the IED sources non-concordant with the *ground-truth IZ*. The inner wedges are for dipoles; the outer wedges are for dSPM. (D) Distance from SOZ (D_{SOZ}) of conv-EEG, HD-EEG and MEG (in mm) for both dipoles and dSPM.

MEG was lower than for conv-EEG ($p = 0.006$, Fig. 4B); while no differences were seen between HD-EEG and MEG ($p = 0.3$) or conv-EEG ($p = 0.1$); and (iii) the overall precision of dSPM was lower than dipoles (Fig. 4C).

3.3.2. Clustered vs. scattered dipoles

We found a proportion of *clustered* dipoles (out of all the *within-coverage* dipoles) equal to 54% for conv-EEG, 88% for HD-EEG and 94% for MEG. For patients showing clusters of dipoles (MEG: 19 patients; HD-EEG: 21 patients; conv-EEG: 17 patients), the E_{Loc} of *clustered* dipoles was lower than the E_{Loc} of *scattered* dipoles in all modalities (*clustered* vs. *scattered*: 21 ± 13.3 vs. 29 ± 14.6 mm for conv-EEG, $p = 0.0081$; 17.5 ± 13.2 vs. 31.8 ± 14.7 mm for HD-EEG, $p = 0.0002$; 14.6 ± 11.5 vs. 28.7 ± 15.4 mm for MEG, $p = 0.0232$). For all modalities, *clustered* dipoles were more precise than *scattered* dipoles ($p < 0.001$; *clustered* vs. *scattered*: 38% vs. 15% for conv-EEG; 51% vs. 12% for HD-EEG; 62% vs. 17% for MEG). Furthermore, the precision of conv-EEG and HD-EEG increased when

Table 2
Localization Error (E_{loc}, in mm), *Distance from Resection* (D_{res}, in mm) and *Resection Percentage* of conv-EEG, HD-EEG and MEG. Results are reported as mean ± standard deviation for both ECD and dSPM solutions. OR: Odds-ratio (calculated for a unit of increase of 10%). CI: Confidence Interval.

			conv-EEG	HD-EEG	MEG
E_{loc} [mm]	ECD		24.7 ± 14.5	19.2 ± 14.2	15.4 ± 12.2
	dSPM		27 ± 15.7	23.2 ± 12.8	20.7 ± 13.1
D_{res} [mm]	ECD	Good-Outcome	22.9 ± 17.7	16.7 ± 17.4	13.4 ± 13.8
		Poor-Outcome	39.4 ± 19.4	25.4 ± 16.5	15.9 ± 14.6
		p-value	<0.001	<0.001	<0.001
	dSPM	Good-Outcome	17.3 ± 11.4	19.5 ± 11.3	16 ± 12.3
		Poor-Outcome	33.2 ± 17.5	30.6 ± 11.4	28.2 ± 17.4
		p-value	<0.001	<0.001	<0.001
Resection Percentage [%]	ECD	Good-Outcome	37	39	58
		Poor-Outcome	7	26	38
		OR (95% CI)	3.2 (−0.31–2.64)	1.2 (−0.19–0.49)	1.2 (−0.16–0.45)
		p-value	0.09	0.36	0.33
	dSPM	Good-Outcome	54	28	51
		Poor-Outcome	0	1	12
		OR (95% CI)	1.8 (−0.08–1.21)	2.1 (−0.16–1.62)	1.4 (−0.02–0.71)
		p-value	0.064	0.088	0.047[a]

[a] *p*-value statistically significant (<0.05).

considering only the *clustered* dipoles instead of the entirety of the dipoles (conv-EEG: $p = 0.0113$; HD-EEG: $p = 0.0089$), while for MEG the increase was not statistically significant ($p = 0.102$).

3.3.3. Concurrent IEDs on MEG and HD-EEG

For the IEDs that were *concurrent* on HD-EEG and MEG, the proportion of outside-coverage dipoles was higher for HD-EEG than for MEG (17% vs. 7%, $p < 0.001$, Fig. 5A). These proportions did not differ from the one observed on the entirety of the dipoles for both MEG ($p = 0.42$) and HD-EEG ($p = 0.12$). For HD-EEG, the E_{Loc} of *concurrent* IEDs (17.5 ± 12.9 mm, Fig. 5B) was smaller than the E_{Loc} estimated from all the HD-EEG IEDs ($p = 0.006$). For MEG, on the contrary, the E_{Loc} of the concurrent IEDs (14.5 ± 11.5 mm, Fig. 5B) did not differ from the entirety of the IEDs (p = 0.80). Furthermore, the localization of *concurrent* IEDs showed higher precision to the *ground-truth IZ* when performed using MEG (61%) than HD-EEG (53%, $p = 0.0077$, Fig. 5C). Finally, the *precision* of HD-EEG increased when considering only the *concurrent* IEDs rather than the entirety of the IEDs ($p = 0.0084$, 7% increase in *precision*). The increase in *precision* of MEG dipoles was not significant ($p = 0.58$).

3.4. Concordance of the IZ with the clinically-defined SOZ

MEG dipoles were closer to the clinically-defined SOZ (D_{SOZ}: 22 ± 10.2 mm) than conv-EEG dipoles (D_{SOZ}: 27.8 ± 15 mm; $p = 0.008$, Fig. 4D). No other differences in D_{SOZ} were found between the non-invasive modalities. The *ground-truth IZ* was closer to the SOZ (D_{SOZ}: 22 ± 14.2 mm) compared to HD-EEG (D_{SOZ}: 25.3 ± 13.4 mm, $p = 0.04$) and conv-EEG dipoles ($p = 0.016$), while no difference was seen with MEG dipoles ($p = 0.08$). Furthermore, we found that the non-invasive modalities did not differ in terms of the gyral-width concordance to the SOZ (MEG: 25%; HD-EEG: 24%; conv-EEG dipoles: 23%), and presented lower concordance than the *ground-truth IZ* (44%). Finally, when using dSPM, the D_{SOZ} of the HD-EEG (30.4 ± 11.5 mm; $p = 0.006$; Fig. 4D) and *ground-truth IZ* (27.9 ± 14.6 mm; $p = 0.009$) increased compared to dipoles.

3.5. Distance of ESI and MSI solutions from resection

For all the investigated modalities, we found that in patients with good outcome the IED sources were closer to the resected volume than in patients with poor outcome (Table 2) for both dipoles (Fig. 6A) and dSPM (Fig. 6B). In patients with good outcomes, who are proof of resection of the EZ, we observed that: (i) the *ground-truth IZ* showed the shortest D_{res} compared to MEG, HD-EEG and conv-EEG dipoles ($p < 0.001$); (ii) among the non-invasive modalities, conv-EEG dipoles were further from the resection compared to MEG dipoles ($p = 0.0084$), but not to HD-EEG dipoles ($p = 0.505$); (iii) the difference between MEG and HD-EEG dipoles in terms of D_{res} did not reach statistical significance ($p = 0.0759$); and (iv) no difference was seen between all non-invasive modalities when using dSPM (Fig. 6B).

3.6. Resection of the IZ as predictor of surgical outcome

The *resection percentage* of the *ground-truth IZ* and MEG IZ (using dSPM) predicted the patient's outcome (iEEG: $p = 0.034$, *odds-ratio*: 1.4; MEG: $p = 0.047$, *odds-ratio*: 1.4; Table 2). On the other hand, the resection of the IZ localized via HD-EEG and conv-EEG tended to predict the outcome but without reaching statistical significance ($p = 0.088$ and $p = 0.064$). For all non-invasive modalities, the *resection percentage* of the IZ localized by dipoles did not predict the outcome (Table 2).

The percentage of resected brain volume did not predict the outcome ($p = 0.17$), as well as the SOZ *resection percentage*, which tended to predict the outcome, but did not reach statistical significance ($p = 0.065$, OR = 1.6). Furthermore, the SOZ *resection percentage* did not correlate with the *resection percentage* of the IZ estimated with any modality ($p > 0.5$, $R < 0.5$).

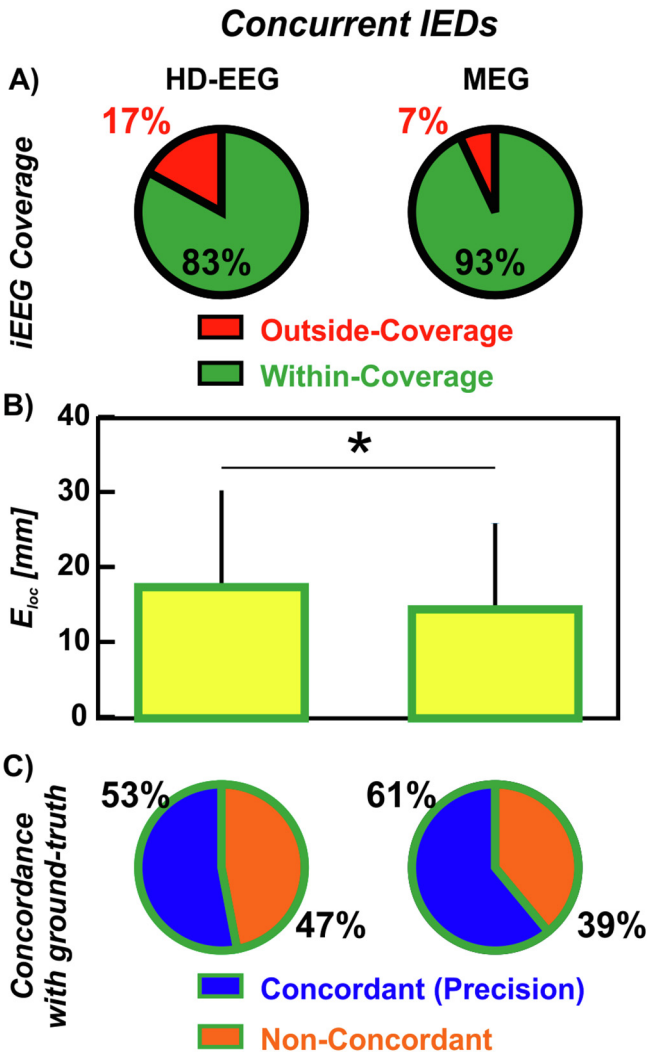

Fig. 5. Non-invasive localization of *concurrent* IEDs on HD-EEG and MEG against ground-truth IZ. (A) Red wedge corresponds to the proportion of dipoles outside the iEEG coverage; green wedge corresponds to the proportion of dipoles within the iEEG coverage. (B) Localization error (E_{loc}) of HD-EEG and MEG dipoles with respect to the iEEG dipoles (in mm). Difference was regarded as significant (*) when the *p*-value was <0.05. (C) Blue wedges correspond to the proportion of dipoles that are concordant with the *ground-truth IZ* at the gyral-width level (out of the *within-coverage* dipoles) or precision. Orange wedges correspond to the dipoles that are non-concordant with the *ground-truth IZ*.

3.7. Concordance of MEG and HD-EEG with other presurgical methods

Ictal EEG and MRI regions for all patients are listed in Table 1. Ictal EEG was diffuse (i.e. included an entire hemisphere or both) in seven cases (29%). HD-EEG and MEG findings were *concordant specific* to the ictal EEG in 79% (n = 19) and 67% (n = 16), respectively, of our patients, and were localized within a lower number of lobes ($p < 0.05$). From the comparison with resection (n = 22), the ictal EEG was *concordant non-specific* in most of the patients (n = 19; 86%; 11 good outcome). In particular, in good outcome patients (n = 13), ictal EEG was *specific* to the resection in only two cases; while, when ictal EEG was *non-specific*, MEG was mostly resected (*resection percentage* ≥ 70%; Kim et al., 2013) in five patients and HD-EEG in three patients.

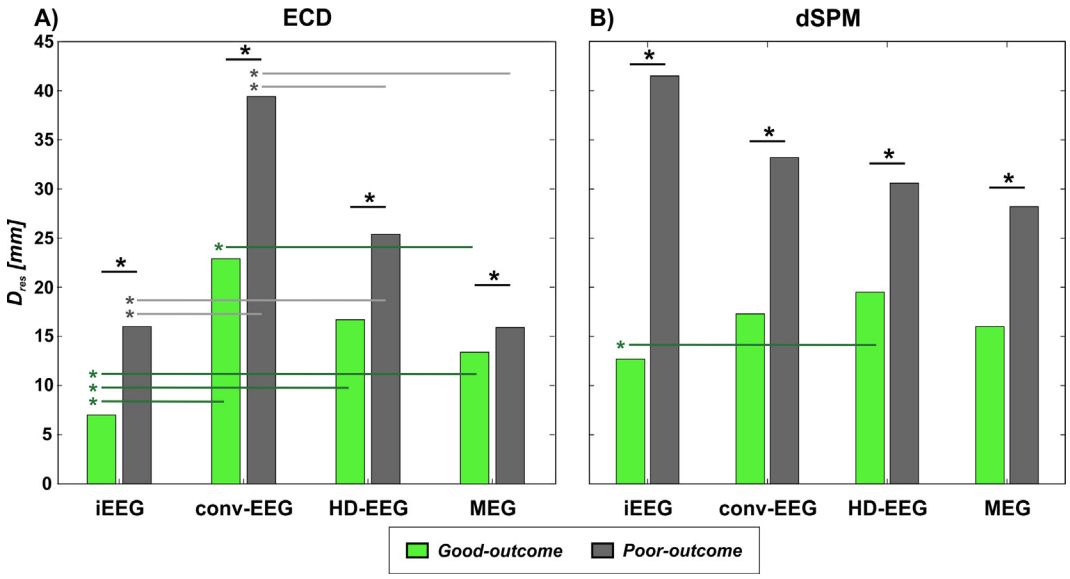

Fig. 6. Distance of IZ (dipoles and dSPM) from the resection (D_{res}) in patients with good vs. poor outcome. IZ is localized using ECD in (A) and dSPM in (B). For each modality, the mean D_{res} (in mm) of the IZ localized in patients with good outcome (green bars) is shown against the mean D_{res} of the IZ localized in patients with poor outcome (grey bars). Significant differences (p-value < 0.05) are indicated with straight lines and an asterisk (*).

Presurgical MRI was negative in seven cases. Within the lesional patients (n = 17), HD-EEG and MEG were *concordant non-specific* to the lesion in most of the cases (HD-EEG: n = 12, 71%; MEG: n = 10, 59%). In the remaining lesional cases, HD-EEG (n = 5) and MEG (n = 7) were *concordant specific*, with the exception of one *discordant* case (poor outcome). In two of the three patients where the lesion was diffuse (i.e. multifocal or large abnormalities in more than two lobes), HD-EEG and MEG were ipsilateral to the lesion and more focal (two lobes).

The MRI lesion was *concordant specific* to the resection in 81% (n = 13) of the lesional cases. In particular, it was *specific* to the resection in 83% (5/6) of the poor outcome cases, and in 80% (8/10) of the good outcomes. When MRI lesion was diffuse and *non-specific* to the resection (n = 3), MEG or HD-EEG regions were mostly resected. Finally, among the non-lesional cases (n = 6, three poor outcome), MEG was mainly resected in four (three good-outcomes) and HD-EEG in two (good outcome) patients.

4. Discussion

In this study, we assessed the localization accuracy and clinical utility of conv-EEG (19–24 electrodes), HD-EEG (72 electrodes) and MEG (306 sensors distributed over 102 locations) in localizing the IZ prior to pediatric epilepsy surgery. Our study details a unique quantitative comparison of these three non-invasive electrophysiological modalities, which are often used to delineate the IZ in surgical patients with MRE. This study adds to the existing literature on the utility of ESI and MSI for epilepsy surgery through the following main findings: (i) MSI presents a higher concordance with the *ground-truth IZ* than ESI (lower E_{loc}, higher gyral-width *precision*), whether this is carried out with conv-EEG or HD-EEG; (ii) clustered sources of IEDs are more precise in localizing the *ground-truth IZ* than scattered ones for both ESI and MSI; (iii) a shorter distance of the IED sources from the resection is associated with good outcome for all the investigated modalities; and (iv) the *resection percentage* of the IZ localized via 306-channel MSI predicts the patient's outcome after surgery. These main findings indicate the higher accuracy and clinical value of MEG in localizing the *ground-truth IZ* non-invasively, but also suggest the possible equally good performance of non-invasive ESI if performed using higher-density EEG systems.

Additionally, this study contributes to the existing body of literature, which compared the iEEG-defined IZ with the ESI/MSI-defined IEDs sources, by addressing two main limitations of previous studies. The first limitation is that the *ground-truth IZ* was defined by the location of the iEEG contacts recording a high rate of IEDs (Birot et al., 2014; Bouet et al., 2012; Gavaret et al., 2009; Huiskamp et al., 2010; Kim et al., 2016; Mégevand et al., 2014) rather than the location of the actual underlying generators. This may introduce an inherent inaccuracy that can compromise the assessment of the ESI or MSI localization error and that is particularly relevant when: (i) the epileptogenic generators are deep and subdural electrodes are used, which exclusively lie on the gyral crown of the cortex; and (ii) depth electrodes are used, since they provide an incomplete and irregular brain coverage. To address this limitation, we defined the *ground-truth IZ* at the source level by applying the same source localization method used for scalp EEG and MEG and localized the sources underlying the IEDs recorded by the iEEG electrodes. The high number of iEEG contacts used to sample all the epileptogenic regions of interest (see Table 1) warranted the reliability of our iEEG source localization (Dümpelmann et al., 2009, 2012), whose validity has been demonstrated even in cases where the iEEG spatial sampling was less extensive or meticulous (Ramantani et al., 2013). Such methodological novelty improves the 3D demarcation of the *ground-truth IZ* and allows performing a direct comparison of the epileptic generators estimated through non-invasive and invasive techniques at the source level. Secondly, this study adds to the existing literature by providing the first quantitative comparison between low-density conv-EEG acquired without head position tracking, and HD-EEG and MEG, which benefit from higher numbers of sensors and accurate EEG-MRI co-registration.

4.1. MEG is more accurate and precise than HD-EEG and conv-EEG in localizing the ground-truth IZ

Our data show that MEG dipoles are more accurate (mean E_{loc} = 15 mm) and precise (*precision* = 59%) than EEG dipoles inde-

pendently if the latter is performed using HD-EEG (E_{loc} = 19 mm; *precision* = 46%) or conv-EEG (E_{loc} = 24 mm; *precision* = 26%). Interestingly, the localization accuracy of the non-invasive modalities did not change when distributed source modeling (i.e. dSPM) was applied (although a decrease in the overall gyral-width precision was observed), prompting the reliability of this source modeling method, despite the fact that it not clinically validated yet. Conventional EEG presented the lowest accuracy and precision in our cohort, which can be explained by the low number of channels and the lack of precise information about the EEG channel location with respect to the patient's head. The low accuracy of conv-EEG may be also due to the selection bias of the present retrospective study, which included only patients who were referred to HD-EEG/MEG after undergoing conv-EEG. Therefore, the exclusion of the cases where conv-EEG already provided definite findings may have underestimated the conv-EEG localization accuracy in this study. Interestingly, HD-EEG outperformed conv-EEG in terms of overall *precision* at the gyral-width level, but not in terms of E_{loc} when the inter-patient variability was considered (mixed-effect ANOVA), using both dipole and distributed sources. These results highlight the low additive value of the 72-channel HD-EEG in our cohort, especially considering its technical complexity with respect to the conv-EEG, which requires shorter setup time, lower frequency of maintenance, and shorter time to review the data (Chu, 2015). These factors are of significant practical importance and must be carefully considered when is to determine the benefits of HD-EEG or MEG with respect to conv-EEG. The superiority of 306-channel MEG also emerged from the analysis at the individual patient level, which pointed out a low proportion of cases (21%) in whom HD-EEG outperformed MEG in terms of localization accuracy, compared to the high proportion of cases in which MEG outperformed HD-EEG (56%). These data indicate the higher accuracy of MEG compared to 72-channel HD-EEG in most of the children in our cohort. However, the small, but non-null, number of cases in which HD-EEG was more accurate than MEG, support the complimentary contribution of these two techniques, especially if we consider the disparity in the number of sensors used between HD-EEG and MEG. The use of HD-EEG systems equipped with up to 256 channels would eliminate the disparity in the number of sensors and possibly in the localization accuracy, which can be enhanced by a higher spatial sampling (Song et al., 2015). The possible equally good performance of HD-EEG compared to MEG is further supported by the dSPM findings, which showed no difference in the localization accuracy between the 306-channel MEG and the 72-channel HD-EEG.

4.2. Clustered dipoles are more accurate in localizing ground-truth IZ than scattered dipoles

Our results show that dipole clustering improves the localization accuracy of IEDs for all three investigated modalities: *clustered* dipoles present a lower E_{loc} and higher gyral-width *precision* than *scattered* ones for conv-EEG (21 vs. 29 mm; 38% vs. 15%), HD-EEG (18 vs. 32 mm; 51% vs. 12%) and MEG (15 vs. 29 mm; 62% vs. 17%). These results suggest that *scattered* dipoles are likely to be false positives, while the combination of multiple dipoles within the same gyrus (*clustered dipoles*) may reflect the presence of a local epileptic neuronal group able to generate epileptiform discharges (Kim et al., 2016). Our MSI results are in line with findings from previous studies, which report a close correlation between clustered dipoles and iEEG-defined IZ (Kim et al., 2016) or SOZ (Mamelak et al., 2002). In addition, our results underlie the importance of clustering for ESI, whether it is performed with a high or low number of sensors: we observed that restricting the analysis to the *clustered* dipoles, rather than to the entirety of the localized sources, enhances the *precision* to the *ground-truth* for both the conv-EEG (38%) and HD-EEG (51%). On the other hand, for MSI, restricting the analysis to the *clustered* dipoles did not improve the *precision* (62%), most likely due to the low proportion of *scattered* dipoles (9%) within the analyzed dipoles.

4.3. Clinical yield of simultaneous HD-EEG and MEG recordings

In line with previous studies (Barkley and Baumgartner, 2003; Iwasaki et al., 2003; Knowlton et al., 1997; Ramantani et al., 2006; Zijlmans et al., 2002), we found a higher number of IEDs on MEG (9.6 IEDs/min) compared to HD-EEG recordings (6.9 IEDs/min). We also observed that most of IEDs were unique to either HD-EEG or MEG, with MEG showing a higher proportion of unique IEDs (73% of the MEG IEDs were not seen on HD-EEG, i.e. *MEG-only*) than HD-EEG (63% of the HD-EEG IEDs were not seen on MEG). This has been observed by previous studies showing that IEDs on MEG are often not seen on simultaneous EEG and vice versa (Lin et al., 2003; Ramantani et al., 2006) and can be explained by the different sensitivities of the two techniques to tangential and radial components of the sources. Furthermore, the high proportion of *HD-EEG-only* and *MEG-only* IEDs indicates how simultaneous HD-EEG/MEG recordings may enhance the yield of IEDs detection compared to single-modality recordings. Our results also show that the localization of *concurrent* IEDs (which constitute a small subset within the entirety of the detected IEDs) improves the localization accuracy and gyral-width *precision* of ESI. This was not the case for MEG, whose E_{loc} did not particularly benefit from restricting the analysis to the *concurrent* IEDs, which is in line with previous findings showing that the localization of *MEG-only* spikes is clinically equivalent to that of *concurrent* spikes on scalp EEG and MEG (Park et al., 2004). This finding suggests that simultaneous HD-EEG/MEG data can particularly help improve the localization accuracy of the IEDs on HD-EEG, by directing the attention on the HD-EEG IEDs that are also visible on MEG.

4.4. Proximity of ESI and MSI solutions to resection is associated with surgical outcome

After estimating the E_{loc}, an important challenge is to determine the clinical value of ESI and MSI with respect to the clinical gold standard of good outcome after resection. For all modalities, we found an association between IED source location, resection and outcome: the closer the IED sources were to the resection, the better was the patient's outcome. These results suggest that ESI and MSI are able to localize epileptogenic generators, whose vicinity to the resection may assist in assessing the patient's prognosis.

In particular, in the cases of proof of EZ resection (good outcome cases), we also observed that: (i) the *ground-truth IZ* provided the best estimate of the EZ with a D_{res} of 7 mm, compared to the non-invasive modalities; and (ii) among the non-invasive modalities, the MEG dipoles were closer to the resection compared to ESI dipoles, whether they were estimated via conv-EEG or HD-EEG (although, for the latter, the difference did not reach full statistical significance, $p = 0.076$), while no difference was seen between MSI and ESI when using dSPM. The first finding suggests that the *ground-truth IZ* estimated via iEEG source localization is a reliable estimator of the EZ in children with MRE. The second finding suggests that MEG dipoles are able to estimate the EZ with higher accuracy than EEG dipoles, which is also in line with the results obtained from the validation against the *ground-truth IZ* (where MEG dipoles showed the lowest E_{loc}). Thus, although the distance of the resection from both ESI and MSI is linked to the patient's outcome (suggesting the promising value of ESI/MSI as EZ estimators), the IED sources estimated through MSI seem to be more accurate in estimating the EZ than ESI, whose higher E_{loc} cannot be overlooked when establishing their clinical value in the

presurgical evaluation. We must also acknowledge that, since the number of channels for MEG was more than three times higher than for HD-EEG, the use of higher-density EEG systems (i.e. 256 channels) may allow reaching similar accuracy of 306-channel MEG. Yet, MEG presents advantages compared to scalp EEG in terms of source localization (i.e. surrounding biological milieu does not distort signals, simplicity of recordings, no bridging of electrodes) (Gaetz et al., 2015), which may confirm MSI superiority to ESI.

4.5. Resection of MSI brain regions predicts patient's outcome

Although the differences in D_{res} between good and poor outcome patients for both ESI and MSI suggest their clinical utility prior to surgery, these group analyses do not help determine the predictive value on an individual patient level. To verify whether ESI or MSI provides clinical information in terms of outcome prediction, we tested whether the *resection percentage* of the ESI/MSI-defined solutions predicted the surgical outcome. First of all, we found that the resection of the *ground-truth IZ* was predictive of outcome: the more the IZ is resected, the higher the patient's probability to achieve good outcome. This result confirms the clinical importance of mapping the IZ during the presurgical evaluation process. More importantly, it provides the first evidence that source localization can be reliably applied to iEEG in the context of IED localization for the prediction of surgical outcome. Furthermore, we found that the resection of the IZ localized via MSI also predicted the outcome: for any 10%-increase in its *resection percentage*, the probability of a good outcome is 1.4 times higher than the probability of a poor outcome (equaling the odds ratio of iEEG; Table 2). This is a fundamental finding that confirms the reliability of MEG to localize the *ground-truth IZ* non-invasively, while preserving its predictive value in terms of outcome. Such predictive value indicates that MSI represents a valid non-invasive alternative to iEEG, particularly for patients unable to handle invasive investigations. This supports the line of evidence of previous prospective MEG studies that showed the presurgical utility of MEG to potentially replace iEEG (Knowlton et al., 2006; Wheless et al., 1999) or optimize its placement (Mamelak et al., 2002; Sutherling et al., 2008). When evaluating the possibility of replacing iEEG with MSI, it is important to consider that: (i) surgery should not necessarily target all the interictal foci localized by MEG, as shown by the non-null D_{res} values in our good-outcome patients and by previous interictal studies (Fischer et al., 2004; Kim et al., 2013), and (ii) iEEG can be only obviated if brain mapping for eloquent cortex localization is not required or can be performed non-invasively (Knowlton et al., 2006).

The IZ localized via HD-EEG and conv-EEG showed a tendency to predict outcome but did not reach significance ($p = 0.088$ and $p = 0.064$). This confirms the lower accuracy of 21- and 72-channel EEG to the *ground-truth IZ* and their lower clinical utility in terms of outcome prediction.

Finally, the association between the IZ resection and the patient's outcome was also strengthened in our cohort by the lack of association between outcome and other potential outcome determinants (resected volume, type of resection, overlap of eloquent cortex with presumed EZ, and SOZ resection). In particular, the lack of association between SOZ resection and outcome suggests that full-head non-invasive source imaging may be complimentary to the current gold standard for resection tailoring given by partial-coverage iEEG (Knowlton et al., 2006).

4.6. Added value of MEG and HD-EEG compared to other non-invasive presurgical methods

An important question typically raised during the presurgical workup of children with MRE is what HD-EEG and MEG may add to other established non-invasive tools. To address this question, we compared our HD-EEG and MEG results with ictal EEG and MRI findings. Our data show that MEG/HD-EEG recordings may be of particular help in patients whose ictal EEG is not focal, since they reduce the extent of the region of interest. We also observed that HD-EEG and MEG potentially add information in terms of resection tailoring with respect to ictal EEG, which seemed to lack in specificity: ictal EEG was specific to the resection only in 15% of the good outcome cases. In 55% of the remaining successful cases, the HD-EEG or MEG regions ended up being targeted for resection. Our results are consistent with previous studies showing that presurgical MEG adds information to video-EEG especially when this is inconclusively localizing (Knowlton et al., 2009; Pataraia et al., 2004; Paulini et al., 2007; Wheless et al., 1999).

Our data also confirmed the pivotal role of presurgical MRI in resection planning: in 81% of the lesional patients, the resection included the MRI abnormality. An exception to this was seen when MRI abnormalities were multifocal or diffuse: in these cases, the HD-EEG or MEG regions ended up being target for resection. Furthermore, the high specificity of the MRI lesion to the resection regardless the surgery success suggests the potential added value of HD-EEG and MEG, which are able to identify additional epileptogenic foci, as confirmed by the high proportion of lesional cases (71% and 59%) where HD-EEG and MEG localized IEDs outside the MRI lesion. Finally, our data indicate that HD-EEG/MEG may particularly facilitates the estimation of the EZ in children with negative MRI, who often end up being regarded ineligible for surgery.

4.7. Limitations and future directions

This study has several limitations that should be considered. There is a disparity in the number of channels between the HD-EEG (72 channels) and MEG (306 sensors), which could affect our source localization findings, since higher spatial sampling offers more accurate EEG localization (Hedrich et al., 2017; Song et al., 2015). Future studies should record and compare simultaneous MEG and HD-EEG recordings using higher-density EEG systems equipped with 128 or 256 channels, which are also available for pediatric use. Furthermore, iEEG, conv-EEG and HD-EEG/MEG data were recorded separately, and the duration of the recordings was different. This impedes investigating the exact correspondence of IEDs between invasive and non-invasive data and warrants future studies using simultaneous recordings. One more limitation of our study is its design, which is limited by its single-center, non-randomized, retrospective nature. Moreover, only patients who underwent HD-EEG/MEG recordings at our center were included in the study introducing a selection bias, since HD-EEG/MEG tests are typically required for the most complicated cases where the EZ is difficult to delineate via previous tests, such as conv-EEG. Future randomized, controlled studies are needed to establish the effects of the investigated modalities on seizure outcome in children undergoing epilepsy surgery. The use of single dipoles does not account for the possibility of multiple underlying generators overlapping in time (Iwasaki et al., 2002); thus, future studies should investigate the use multiple ECDs in comparison with distributed source models. Furthermore, when interpreting the results on the concordance between the IZ and the clinically-defined SOZ, we must consider that the SOZ was defined by the location of the recording iEEG contacts, rather than by the underlying sources. This possibly explains the low concordance and high distance (Fig. 4D) of the IZ to the SOZ. The possible propagation of IEDs from a primary epileptogenic generator toward less epileptogenic areas, as previously reported using both invasive (Alarcon et al., 1997; Tamilia et al., 2018) and non-invasive techniques (Tanaka et al., 2012), may lead to a misallocation of the IED sources; thus, further studies are prompted to investigate the IED propagation via ESI and

MSI with respect to the EZ. Finally, recent findings on the superiority of interictal high frequency oscillations (HFOs) to the IEDs in the estimation of the EZ (Jacobs et al., 2010; Tamilia et al. 2018) and on their detectability via non-invasive modalities (Papadelis et al. 2016; Tamilia et al. 2017; Van Klink et al. 2018) prompt future quantitative studies that compare non-invasively localized IEDs and HFOs in terms of epilepsy surgery prediction.

5. Conclusions

The present study quantitatively assessed the localization accuracy of presurgical source imaging performed via conv-EEG, HD-EEG and MEG in pediatric patients with MRE. Our data show that MSI (306-channel MEG) is more accurate (E_{loc} = 15 mm) than ESI in localizing the IZ, whether ESI is carried out with conv-EEG (19–24 channels, E_{loc} = 25 mm) or 72-channel HD-EEG (E_{loc} = 19 mm). The proximity of the non-invasively estimated IZ to the resection was linked to the surgical outcome, demonstrating that ESI and MSI solutions can be interpreted as presurgical indicators of the EZ location. This contribution is not limited to the use of highly sophisticated techniques, such as HD-EEG or MEG, but also when ESI is performed on conv-EEG data, typically available in all epilepsy centers. Furthermore, the amount of the MEG IZ that was resected was able to predict the patient's probability of good or poor outcome, demonstrating the clinical utility of MEG in terms of outcome prediction for children with MRE undergoing surgery.

Acknowledgements

This work was supported by the American Epilepsy Society Junior Investigator Research Award (PI: Papadelis; 2015), the Faculty Career Development Grant from Harvard Medical School (PI: Papadelis; 2014); the R21NS101373-01A1 from the National Institute of Neurological Disorders & Stroke (PIs: Papadelis and Stufflebeam), and the Boston Children's Hospital Intellectual and Development Disabilities Research Center (BCH IDDRC, 1U54HD090255).

Conflict of interest

None of the authors have potential conflicts of interest to be disclosed.

Appendix A. Supplementary material

Supplementary data to this article can be found online at https://doi.org/10.1016/j.clinph.2019.01.009.

References

Abdallah C, Maillard LG, Rikir E, Jonas J, Thiriaux A, Gavaret M, et al. Localizing value of electrical source imaging: Frontal lobe, malformations of cortical development and negative MRI related epilepsies are the best candidates. NeuroImage Clin 2017;16:319–29. https://doi.org/10.1016/j.nicl.2017.08.009.

Alarcon G, Garcia Seoane JJ, Binnie CD, Martin Miguel MC, Juler J, Polkey CE, et al. Origin and propagation of interictal discharges in the acute electrocorticogram. Implications for pathophysiology and surgical treatment of temporal lobe epilepsy. Brain 1997;120(12):2259–82.

Almubarak S, Alexopoulos A, Von-Podewils F, Wang ZI, Kakisaka Y, Mosher JC, et al. The correlation of magnetoencephalography to intracranial EEG in localizing the epileptogenic zone: a study of the surgical resection outcome. Epilepsy Res 2014;108(9):1581–90. https://doi.org/10.1016/j.eplepsyres.2014.08.016.

Bagic AI, Knowlton RC, Rose DF, Ebersole JS, ACMEGS Clinical Practice Guideline (CPG) Committee. American clinical magnetoencephalography society clinical practice guideline 1: recording and analysis of spontaneous cerebral activity. J Clin Neurophysiol 2011;28(4):348–54. https://doi.org/10.1097/WNP.0b013e3182272fed.

Bailet LL, Turk WR. The impact of childhood epilepsy on neurocognitive and behavioral performance: a prospective longitudinal study. Epilepsia 2000;41(4):426–31.

Barkley GL, Baumgartner C. MEG and EEG in epilepsy. J Clin Neurophysiol 2003;20(3):163–78.

Barth DS, Sutherling W, Engel J, Beatty J. Neuromagnetic localization of epileptiform spike activity in the human brain. Science 1982;218(4575):891–4.

Bast T, Oezkan O, Rona S, Stippich C, Seitz A, Rupp A, et al. EEG and MEG source analysis of single and averaged interictal spikes reveals intrinsic epileptogenicity in focal cortical dysplasia. Epilepsia 2004;45(6):621–31. https://doi.org/10.1111/j.0013-9580.2004.56503.x.

Birot G, Spinelli L, Vulliémoz S, Mégevand P, Brunet D, Seeck M, et al. Head model and electrical source imaging: a study of 38 epileptic patients. NeuroImage Clin 2014;5:77–83. https://doi.org/10.1016/j.nicl.2014.06.005.

Bouet R, Jung J, Delpuech C, Ryvlin P, Isnard J, Guenot M, et al. Towards source volume estimation of interictal spikes in focal epilepsy using magnetoencephalography. Neuroimage 2012;59(4):3955–66. https://doi.org/10.1016/j.neuroimage.2011.10.052.

Brodbeck V, Spinelli L, Lascano AM, Wissmeier M, Vargas MI, Vulliemoz S, et al. Electroencephalographic source imaging: a prospective study of 152 operated epileptic patients. Brain 2011;134(10):2887–97. https://doi.org/10.1093/brain/awr243.

Chatrian GE. A glossary of terms most commonly used by clinical electroencephalographers. Electroencephalogr Clin Neurophysiol. 1974;37:538–48.

Chu CJ. High density EEG—What do we have to lose? Clin Neurophysiol 2015;126(3):433–4. https://doi.org/10.1016/j.clinph.2014.07.003.

Cowan LD, Bodensteiner JB, Leviton A, Doherty L. Prevalence of the epilepsies in children and adolescents. Epilepsia 1989;30(1):94–106.

Dale AM, Fischl B, Sereno MI. Cortical surface-based analysis: I. Segmentation and surface reconstruction. Neuroimage 1999;9(2):179–94. https://doi.org/10.1006/nimg.1998.0395.

Dale AM, Liu AK, Fischl BR, Buckner RL, Belliveau JW, Lewine JD. Dynamic statistical parametric mapping: combining fMRI and MEG for high-resolution imaging of cortical activity. Neuron 2000;26(1):55–67.

Diekmann V, Becker W, Jürgens R, Grözinger B, Kleiser B, Richter HP, et al. Localisation of epileptic foci with electric, magnetic and combined electromagnetic models. Electroencephalogr Clin Neurophysiol 1998;106(4):297–313.

Dümpelmann M, Fell J, Wellmer J, Urbach H, Elger CE. 3D source localization derived from subdural strip and grid electrodes: a simulation study. Clin Neurophysiol 2009;120(6):1061–9. https://doi.org/10.1016/j.clinph.2009.03.014.

Dümpelmann M, Ball T, Schulze-Bonhage A. sLORETA allows reliable distributed source reconstruction based on subdural strip and grid recordings. Hum Brain Mapp 2012;33(5):1172–88. https://doi.org/10.1002/hbm.21276.

Engel J, Van Ness PC, Rasmussen TB, Ojemann LM. Outcome with respect to epileptic seizures. In: Engel J, editor. Surgical treatment of epilepsies. 2nd ed. New York, NY: Raven Press; 1993. p. 609–21.

Englot DJ, Nagarajan SS, Imber BS, Raygor KP, Honma SM, Mizuiri D, et al. Epileptogenic zone localization using magnetoencephalography predicts seizure freedom in epilepsy surgery. Epilepsia 2015;56(6):949–58. https://doi.org/10.1111/epi.13002.

Fischer MJ, Scheler G, Stefan H. Utilization of magnetoencephalography results to obtain favourable outcomes in epilepsy surgery. Brain 2004;128(1):153–7. https://doi.org/10.1093/brain/awh333.

Gaetz W, Gordon RS, Papadelis C, Fujiwara H, Rose DF, Edgar JC, Schwartz ES, Roberts TP. Magnetoencephalography for clinical pediatrics: recent advances in hardware, methods, and clinical applications. J Pediatr Epilepsy 2015;04(04):139–55.

Gavaret M, Trébuchon A, Bartolomei F, Marquis P, McGonigal A, Wendling F, et al. Source localization of scalp-EEG interictal spikes in posterior cortex epilepsies investigated by HR-EEG and SEEG. Epilepsia 2009;50(2):276–89. https://doi.org/10.1111/j.1528-1167.2008.01742.x.

Gramfort A, Papadopoulo T, Olivi E, Clerc M. OpenMEEG: opensource software for quasistatic bioelectromagnetics. Biomed Eng Online 2010;9(1):45. https://doi.org/10.1186/1475-925X-9-45.

Hamalainen M, Hari R, Ilmoniemi RJ, Knuutila J, Lounasmaa OV. Magnetoencephalography – theory, instrumentation, and applications to noninvasive studies of the working human brain. Rev Mod Phys 1993;65(2):413–97.

Hari R, Puce A. MEG-EEG primer. Oxford University Press; 2017.

Hari R, Baillet S, Barnes G, Burgess R, Forss N, Gross J, et al. IFCN-endorsed practical guidelines for clinical magnetoencephalography (MEG). Clin Neurophysiol 2018;129(8):1720–47.

Hedrich T, Pellegrino G, Kobayashi E, Lina JM, Grova C. Comparison of the spatial resolution of source imaging techniques in high-density EEG and MEG. NeuroImage 2017;157:531–44. https://doi.org/10.1016/j.neuroimage.2017.06.022.

Holmes CJ, Hoge R, Collins DL, Woods R, Toga AW, Evans AC. Enhancement of MR images using registration for signal averaging. J Comput Assist Tomogr 1998;22(2):324–33.

Huiskamp G, Agirre-Arrizubieta Z, Leijten F. Regional differences in the sensitivity of MEG for interictal spikes in epilepsy. Brain Topogr 2010;23(2):159–64. https://doi.org/10.1007/s10548-010-0134-1.

Iwasaki M, Nakasato N, Shamoto H, Nagamatsu KI, Kanno A, Hatanaka K, et al. Surgical implications of neuromagnetic spike localization in temporal lobe epilepsy. Epilepsia 2002;43(4):415–24.

Iwasaki M, Nakasato N, Shamoto H, Yoshimoto T. Focal magnetoencephalographic spikes in the superior temporal plane undetected by scalp EEG. J Clin Neurosci 2003;10(2):236–8.

Jacobs J, Zijlmans M, Zelmann R, Chatillon CÉ, Hall J, Olivier A, Dubeau F, Gotman J. High-frequency electroencephalographic oscillations correlate with outcome of epilepsy surgery. Ann Neurol 2010;67(2):209–20.

Kim D, Joo EY, Seo DW, Kim MY, Lee YH, Kwon HC, et al. Accuracy of MEG in localizing irritative zone and seizure onset zone: quantitative comparison between MEG and intracranial EEG. Epilepsy Res 2016;127:291–301. https://doi.org/10.1016/j.eplepsyres.2016.08.013.

Kim H, Kankirawatana P, Killen J, Harrison A, Oh A, Rozzelle C, et al. Magnetic source imaging (MSI) in children with neocortical epilepsy: surgical outcome association with 3D post-resection analysis. Epilepsy Res 2013;106(1–2):164–72. https://doi.org/10.1016/j.eplepsyres.2013.04.004.

Knake S, Halgren E, Shiraishi H, Hara K, Hamer HM, Grant PE, et al. The value of multichannel MEG and EEG in the presurgical evaluation of 70 epilepsy patients. Epilepsy Res 2006;69(1):80–6. https://doi.org/10.1016/j.eplepsyres.2006.01.001.

Knowlton RC, Laxer KD, Aminoff MJ, Roberts TPL, Wong STC, Rowley HA. Magnetoencephalography in partial epilepsy: clinical yield and localization accuracy. Ann Neurol 1997;42(4):622–31. https://doi.org/10.1002/ana.410420413.

Knowlton RC, Elgavish R, Howell J, Blount J, Burneo JG, Faught E, et al. Magnetic source imaging versus intracranial electroencephalogram in epilepsy surgery: a prospective study. Ann Neurol 2006;59(5):835–42. https://doi.org/10.1002/ana.20857.

Knowlton RC, Elgavish RA, Limdi N, Bartolucci A, Ojha B, Blount J, et al. Functional imaging: I. Relative predictive value of intracranial electroencephalography. Ann Neurol 2008a;64(1):25–34. https://doi.org/10.1002/ana.21389.

Knowlton RC, Elgavish RA, Bartolucci A, Ojha B, Limdi N, Blount J, et al. Functional imaging: II. Prediction of epilepsy surgery outcome. Ann Neurol 2008b;64:35–41. https://doi.org/10.1002/ana.21419.

Knowlton RC, Razdan SN, Limdi N, Elgavish RA, Killen J, Blount J, Burneo JG, Ver Hoef L, Paige L, Faught E, Kankirawatana P. Effect of epilepsy magnetic source imaging on intracranial electrode placement. Ann Neurol 2009;65(6):716–23.

Lantz G, De Peralta RG, Spinelli L, Seeck M, Michel CM. Epileptic source localization with high density EEG: how many electrodes are needed? Clin Neurophysiol 2003;114(1):63–9.

Lascano AM, Perneger T, Vulliemoz S, Spinelli L, Garibotto V, Korff CM, et al. Yield of MRI, high-density electric source imaging (HD-ESI), SPECT and PET in epilepsy surgery candidates. Clin Neurophysiol 2016;127(1):150–5. https://doi.org/10.1016/j.clinph.2015.03.025.

Leijten FS, Huiskamp GJM, Hilgersom I, van Huffelen AC. High-resolution source imaging in mesiotemporal lobe epilepsy: a comparison between MEG and simultaneous EEG. J Clin Neurophysiol 2003;20(4):227–38.

Lin YY, Shih YH, Hsieh JC, Yu HY, Yiu CH, Wong TT, et al. Magnetoencephalographic yield of interictal spikes in temporal lobe epilepsy: comparison with scalp EEG recordings. Neuroimage 2003;19(3):1115–26.

Mamelak AN, Lopez N, Akhtari M, Sutherling WW. Magnetoencephalography-directed surgery in patients with neocortical epilepsy. J Neurosurg 2002;97(4):865–73. https://doi.org/10.3171/jns.2002.97.4.0865.

Mégevand P, Seeck M. Electroencephalography, magnetoencephalography and source localization: their value in epilepsy. Curr Opin Neurol 2018;31(2):176–83. https://doi.org/10.1097/WCO.0000000000000545.

Mégevand P, Spinelli L, Genetti M, Brodbeck V, Momjian S, Schaller K, et al. Electric source imaging of interictal activity accurately localises the seizure onset zone. J Neurol Neurosurg Psychiatry 2014;85(1):38–43. https://doi.org/10.1136/jnnp-2013-305515.

Murakami H, Wang ZI, Marashly A, Krishnan B, Prayson RA, Kakisaka Y, et al. Correlating magnetoencephalography to stereo-electroencephalography in patients undergoing epilepsy surgery. Brain 2016;139(11):2935–47. https://doi.org/10.1093/brain/aww215.

Nakasato N, Levesque MF, Barth DS, Baumgartner C, Rogers RL, Sutherling WW. Comparisons of MEG, EEG, and ECoG source localization in neocortical partial epilepsy in humans. Electroencephalogr Clin Neurophysiol 1994;91(3):171–8.

Nissen IA, Stam CJ, Citroen J, Reijneveld JC, Hillebrand A. Preoperative evaluation using magnetoencephalography: experience in 382 epilepsy patients. Epilepsy Res 2016;124:23–33.

Önal Ç, Otsubo H, Araki T, Chitoku S, Ochi A, Weiss S, et al. Complications of invasive subdural grid monitoring in children with epilepsy. J Neurosurg 2003;98(5):1017–26. https://doi.org/10.3171/jns.2003.98.5.1017.

Ono M, Kubik S, Abernathey CD. Atlas of the cerebral sulci. Stuttgart: Georg Thieme; .

Ossenblok P, De Munck JC, Colon A, Drolsbach W, Boon P. Magnetoencephalography is more successful for screening and localizing frontal lobe epilepsy than electroencephalography. Epilepsia 2007;48(11):2139–49. https://doi.org/10.1111/j.1528-1167.2007.01223.x.

Papadelis C, Tamilia E, Stufflebeam S, Grant PE, Madsen JR, Pearl PL, et al. Interictal high frequency oscillations detected with simultaneous magnetoencephalography and electroencephalography as biomarker of pediatric epilepsy. Jove J Vis Exp 2016(118). https://doi.org/10.3791/54883.

Park HM, Nakasato N, Iwasaki M, Shamoto H, Tominaga T, Yoshimoto T. Comparison of magnetoencephalographic spikes with and without concurrent electroencephalographic spikes in extratemporal epilepsy. Tohoku J Exp Med 2004;203(3):165–74.

Park CJ, Seo JH, Kim D, Abibullaev B, Kwon H, Lee YH, et al. EEG source imaging in partial epilepsy in comparison with presurgical evaluation and magnetoencephalography. J Clin Neurol 2015;11(4):319–30. https://doi.org/10.3988/jcn.2015.11.4.319.

Pataraia E, Simos PG, Castillo EM, Billingsley RL, Sarkari S, Wheless JW, Maggio V, Maggio W, Baumgartner JE, Swank PR, Breier JI. Does magnetoencephalography add to scalp video-EEG as a diagnostic tool in epilepsy surgery? Neurology 2004;62(6):943–8.

Paulini A, Fischer M, Rampp S, Scheler G, Hopfengärtner R, Kaltenhäuser M, Dörfler A, Buchfelder M, Stefan H. Lobar localization information in epilepsy patients: MEG—a useful tool in routine presurgical diagnosis. Epilepsy Res 2007;76(2–3):124–30.

Pellegrino G, Hedrich T, Chowdhury RA, Hall JA, Dubeau F, Lina JM, et al. Clinical yield of magnetoencephalography distributed source imaging in epilepsy: a comparison with equivalent current dipole method. Hum Brain Mapp 2018;39(1):218–31. https://doi.org/10.1002/hbm.23837.

Prabhu S, Mahomed N. Imaging of intractable paediatric epilepsy. S Afr J Radiol 2015;19(2):1–10.

Ramantani G, Boor R, Paetau R, Ille N, Feneberg R, Rupp A, Boppel T, Scherg M, Bast T. MEG versus EEG: influence of background activity on interictal spike detection. J Clin Neurophysiol 2006;23(6):498–508.

Ramantani G, Cosandier-Rimélé D, Schulze-Bonhage A, Maillard L, Zentner J, Dümpelmann M. Source reconstruction based on subdural EEG recordings adds to the presurgical evaluation in refractory frontal lobe epilepsy. Clin Neurophysiol 2013;124(3):481–91. https://doi.org/10.1016/j.clinph.2012.09.001.

Rikir E, Koessler L, Gavaret M, Bartolomei F, Colnat-Coulbois S, Vignal JP, et al. Electrical source imaging in cortical malformation–related epilepsy: a prospective EEG-SEEG concordance study. Epilepsia 2014;55(6):918–32. https://doi.org/10.1111/epi.12591.

Rosenow F, Lüders H. Presurgical evaluation of epilepsy. Brain 2001;124(9):1683–700.

Russo A, Jayakar P, Lallas M, Miller I, Hyslop A, Korman B, et al. The diagnostic utility of 3D electroencephalography source imaging in pediatric epilepsy surgery. Epilepsia 2016;57(1):24–31. https://doi.org/10.1111/epi.13228.

Ryvlin P, Cross JH, Rheims S. Epilepsy surgery in children and adults. Lancet Neurol 2014;13(11):1114–26. https://doi.org/10.1016/S1474-4422(14)70156-5.

Shah R, Botre A, Udani V. Trends in pediatric epilepsy surgery. Indian J Pediatr 2015;82(3):277–85. https://doi.org/10.1007/s12098-014-1660-8.

Song J, Davey C, Poulsen C, Luu P, Turovets S, Anderson E, et al. EEG source localization: sensor density and head surface coverage. J Neurosci Meth 2015;256:9–21. https://doi.org/10.1016/j.jneumeth.2015.08.015.

Stefan H, Hummel C, Scheler G, Genow A, Druschky K, Tilz C, et al. Magnetic brain source imaging of focal epileptic activity: a synopsis of 455 cases. Brain 2003;126(11):2396–405. https://doi.org/10.1093/brain/awg239.

Sutherling WW, Mamelak AN, Thyerlei D, Maleeva T, Minazad Y, Philpott L, Lopez N. Influence of magnetic source imaging for planning intracranial EEG in epilepsy. Neurology 2008;71(13):990–6.

Tadel F, Baillet S, Mosher JC, Pantazis D, Leahy RM. Brainstorm: a user-friendly application for MEG/EEG analysis. Comput Intell Neurosci 2011;2011:8. https://doi.org/10.1155/2011/879716.

Tamilia E, Madsen JR, Grant PE, Pearl PL, Papadelis C. Current and emerging potential of magnetoencephalography in the detection and localization of high-frequency oscillations in epilepsy. Front Neurol 2017;8:14.

Tamilia E, Park EH, Percivati S, Bolton J, Taffoni F, Peters JM, et al. Surgical resection of ripple onset predicts outcome in pediatric epilepsy. Ann Neurol 2018. https://doi.org/10.1002/ana.25295.

Tanaka N, Grant PE, Suzuki N, Madsen JR, Bergin AM, Hämäläinen MS, et al. Multimodal imaging of spike propagation: a technical case report. AJNR Am J Neuroradiol 2012;33(6):E82–4. https://doi.org/10.3174/ajnr.A2701.

Tanaka N, Papadelis C, Tamilia E, Madsen JR, Pearl PL, Stufflebeam SM. Magnetoencephalographic mapping of epileptic spike population using distributed source analysis: comparison with intracranial electroencephalographic spikes. J Clin Neurophysiol 2018a;35(4):339–45. https://doi.org/10.1097/WNP.0000000000000476.

Tanaka N, Papadelis C, Tamilia E, AlHilani M, Madsen JR, Pearl PL, et al. Magnetoencephalographic spike analysis in patients with focal cortical dysplasia: what defines a “Dipole Cluster”? Pediatr Neurol 2018b;83:25–31. https://doi.org/10.1016/j.pediatrneurol.2018.03.004.

Uusitalo MA, Ilmoniemi RJ. Signal-space projection method for separating MEG or EEG into components. Med Biol Eng Comput 1997;35(2):135–40.

Van Klink N, Mol A, Ferrier C, Hillebrand A, Huiskamp G, Zijlmans M. Beamforming applied to surface EEG improves ripple visibility. Clin Neurophysiol 2018;129(1):101–11.

Velmurugan J, Nagarajan SS, Mariyappa N, Ravi SG, Thennarasu K, Mundlamuri RC, et al. Magnetoencephalographic imaging of ictal high-frequency oscillations (80–200 Hz) in pharmacologically resistant focal epilepsy. Epilepsia 2018;59(1):190–202.

Wheless JW, Willmore LJ, Breier JI, Kataki M, Smith JR, King DW, Meador KJ, Park YD, Loring DW, Clifton GL, Baumgartner J. A comparison of magnetoencephalography, MRI, and V-EEG in patients evaluated for epilepsy surgery. Epilepsia 1999;40(7):931–41.

Zijlmans M, Huiskamp GM, Leijten FS, van der Meij WM, Wieneke G, van Huffelen AC. Modality-specific spike identification in simultaneous magnetoencephalography/electroencephalography: a methodological approach. J Clin Neurophysiol 2002;19(3):183–91.